Analysis of the Full-Scale Technical Integration of an Hyperloop System

Hyperloop Manchester
Full-scale Technical
7001 Words
Hyperloop-manchester.com

This document is a summary of Hyperloop Manchester's research into the **Full-Scale Technical** integration of an Hyperloop system. Our determined team of student engineers have taken a materials-focused approach when considering tunnel construction and discussed potential concerns with inducing and maintaining low vacuum conditions.

Hyperloop Manchester is a student-led team which aims to compete in international Hyperloop competitions organised by esteemed institutions and to share our knowledge with people across the globe. The team was founded in 2019 and has rapidly recruited a wide range of brilliant-minded members. Today, Hyperloop Manchester has 80 team members and 50 alumni from around the world.

Statement of Contribution

Eve Brittain – *Materials Science and Engineering*
Team Lead/Materials Engineer
Wrote chapters 1, 2, 3, 4.3

Nancy Keegan – *Materials Science and Engineering*
Co-Lead/Materials Engineer
Wrote chapter 4.2

Dhillon Dhass Zhao
Mechanical Engineering
Vacuums Engineer
Wrote chapters 2, 4.4.1

Jean-Thomas Valls
Mechanical Engineering
Vacuums Engineer
Wrote chapters 2, 4.4.2

Madeline Hill – *Materials Science and Engineering*
Materials Engineer
Wrote chapters 2, 4.1

Tibault Dary-Alabaster
Mechanical Engineering
Vacuums Engineer
Wrote chapters 2, 4.4.1

Douaya Junior Diety – *Mechanical Engineering*
Vacuums Engineer
Wrote chapters 2, 4.4.2

CONTENTS

1. **Abstract** (239 words)

Hyperloop Manchester's research into the technical aspects of full-scale integration of an Hyperloop system aims to unpack two major limitations associated with the system. Which materials can withstand these conditions while remaining economically viable for large scale implementation? And how can we induce and sustain low vacuum conditions? With this research, we hope to propose potential solutions to these technical limitations and bring us one step closer to making Hyperloop a reality.

It was concluded that a thick high strength low alloy steel with an insulative and corrosion resistant exterior polyimide coating is both an effective and affordable approach to designing and constructing an Hyperloop tunnel. The reason for the vacuum system is also important when attempting to justify complex engineering systems from an economic perspective, this has therefore been discussed. A thorough comparison between pre-existing rotary vane pump vacuum systems and a novel design of our own was conducted in an effort to identify what further research must be done in order to conclude what approach is optimal for the system.

Therefore, a practical approach towards the design of a vacuum system must be taken that can be implemented sustainably and pragmatically within the entire infrastructure. This would consider the type of constituent equipment used, the installation of said equipment, and the long-term functionality of said equipment. Our research aims to establish a functional relationship between vacuum percentage, time to reach that level, and financial and energetic costs.

2. Introduction

To start, it's important to consider the location of the tunnel itself. The tunnel-encasing of the Hyperloop pods is of the utmost importance as their pods cannot function without this. A faulty tunnel poses a great risk to the passengers and the function of the pods. Therefore, researching all risks that threaten the performance and cause potentially catastrophic outcomes must be researched with mitigating solutions provided. The system's design and construction depend on an array of factors, such as location, and terrain with risk factors posed. This document will examine the implications of constructing the Hyperloop system in an overground vs. underground tunnel and a conclusion as to why the former is preferred. The main research areas will investigate the economic, environmental and technicalities the tunnel poses for the two scenarios.

An additional concern that has prompted research is that a vacuum tunnel faces risk of collapse. The external pressure exerted on the tunnel as a result of its sub-atmospheric internal pressure introduces stresses in the tunnel walls that may lead to catastrophic failure. Both the tunnel's dimensions and materials are determining factors in whether it is susceptible to collapse during depressurisation. This incentivised research into tunnel building materials specifically, cross-examining their properties and affordability with respect to each other.

As well as the threat of vacuum buckling, environmental degradation is always a concern for engineering components in service. Environmental factors from temperature changes to rain fall pose a threat to the longevity of a component, undermining our ability to predict when they become unsafe. Corrosion protection was therefore a topic of research.

The basic idea behind the revolutionary technology of Hyperloop is to considerably reduce friction in order for the pod to reach a very high velocity. This is achieved through the combination of magnetic-levitation and reduced pressure tunnels. These two characteristics are the pillars of Hyperloop. However, very little information on the Hyperloop vacuum tunnel is available, which seems problematic compared to its importance. In this regard, the following study will cover the research on the generation of a partial vacuum in the Hyperloop tunnel.

A practical approach towards the design of a vacuum system must be taken that can be implemented sustainably and pragmatically within the entire infrastructure. This would consider the type of constituent equipment used, the installation of said equipment, and the long-term functionality of said equipment. A functional relationship of vacuum percentage, time to reach that level, and both financial and energetic costs must be established.

There are many industries that already use vacuum conditions. the most sophisticated ones are found in the aerospace industry (high vacuum) and the study of particles (ultra-high vacuum). These extreme conditions are realised with the help of vacuum pumps. There is a consequent variety of vacuum pumps that can be classified with regard to their size and type.

Concerning our Hyperloop tunnel model, we are aiming to achieve a 1% atm vacuum. This can be identified as a low or rough vacuum (LV). We then have to find a suitable pumping mechanism for our vacuum condition.

3. Methodology

This research was conducted using published academic literature and additional online resources. MatLab was used to plot data to visualize data from calculations.

4. Research & Discussion

4.1. Analysis of Over-Ground vs Underground Tunnel Design Challenges and Risks

Environmental Factors

These are issues that are implicated due to the placement of the tunnel which cannot be avoided due to not being in our control. However, mitigation to risk may be employed for certain scenarios. These issues involve natural disasters, geological hazards, adverse weather conditions and human activity. Underground and overground may be influenced by the same risk however, each scenario will have a few that just impacts them.

Overground issues and mitigation

Many natural occurrences put an overground tunnel at risk, with many leading to catastrophic failure unless mitigation is employed. Severe weather events can cause extreme damage to the tunnel, with moderate winds causing vibrations and inflicting damage to the structural integrity of the tunnel. Placing this overground tunnel on sturdy pylons helps to mitigate the risk imposed and provides other benefits to the tunnel such as earthquake protection and buoyancy to gravity. This security for earthquakes is due to the elevation preventing a large amount of ground motion from experience, as shorter stiffer structures experience greater ground motion. Therefore, these pylons must have the flexibility to allow greater mitigation for stronger earthquakes. The terrain offers limitations to the mitigation the pylons can provide, as harder soils reduce the ground motion with soft soils amplify the seismic waves. [1] To offer greater protection from the hazard, seismic isolation systems can be employed at the base of the pylons reducing the amount of energy transferred into the pylons. As the tunnel already being made from a conductive steel tunnel there is mitigation already to lightning strikes. Coating this tunnel with a corrosive protection layer will be necessary to protect it from saline environments which gives added protection for the tunnel which will be made from HSLA steel (see 4.3.3.). The tunnel is placed on pylons means it can be built over roads and other man-made infrastructure, allowing it to be integrated without much disruption to society. Incorporating solar panels onto the tunnel allows another use for the tunnel to make the building greener and if the tunnel follows roads already built this should help prevent too much destruction to wildlife. [2]

Underground issues and mitigation

Creating a tunnel underground is not a novel area as it's been seen in infrastructure for some time such as underground rail systems and the Euro tunnel. These tunnels need a lot of infrastructure to prevent collapse, especially in earthquake-prone zones and places at risk of flood due to the tunnel being placed below the water table. The tunnels themselves should automatically be protected from shockwaves as they're held firmly in place in the ground, however, the risk is posed by permanent ground movement caused by earthquakes which unfortunately can't be mitigated. This isn't an issue for current underground rail circuits as the ground movement is hyper-localised therefore, the risk imposed on people is slim. [3] This is a different issue for the Hyperloop tunnel, as a small

compromise in the structure of the tunnel would result in a catastrophic implosion. There isn't an obvious solution to this risk posed, therefore, making the underground solution seem of greater risk. The tunnel would be situated in a saline environment therefore, the protective coating against corrosion would be necessary. The other issues mentioned for the overground scenario wouldn't be an issue due to the underground placement. Flooding poses a risk, especially in hurricane-prone areas, pumping systems can be integrated to help prevent a huge amount of water from building up. [2] [4]

Economical

An overground tunnel on pylons is a much cheaper, quicker, and simpler infrastructure than boring an underground tunnel. Boring equipment has a lifetime that may not extend to the full range of the tunnels, as Hyperloop is designed for large-distance cross-country travelling. Underground systems haven't been designed for long-distance as they are for within-city travel where there is no option but to place it underground. Also, with new environmental regulations appropriate life cycle assessments must be done to find the most environmentally friendly and economically viable construction route from materials sourced to disposable materials at their end of life. [5] However, overground seems to be less risky as it doesn't have the requirements of excavation, reinforcement and drainage as an underground tunnel would. The over ground may cause more disruption to surrounding areas during construction, it would be completed in a quicker time frame than an underground system. More land will be required for an overground tunnel, increasing cost, however, an underground poses a risk to existing infrastructure and utilities. [6] In the future, the overground tunnel will be easier to modify and expand making it attainable to keep up with modern technologies, whilst the underground tunnel doesn't have as much room for manoeuvre. Hyperloop offers a sustainable mode for travelling which tackles one of the biggest issues in current times. Justifying the vast amount of money Hyperloop would cost is an issue that needs to be overcome.

Technical

Many technicalities impose the risk of catastrophic failure on the Hyperloop plus risk to the life of passengers travelling on the Hyperloop. Making escape routes is necessary for the health and safety of this mode of transport. However, adding the need for escape routes introduces more points for potential failure which again increases cost and risk. Above-ground re-pressurisation vents can be introduced serving also as a point of escape. [7] Under-ground there is a restriction in the ability to install emergency vents and making infrastructure to enable these vents will dramatically increase costs. [8] The above-ground scenario also has risks posed by vandalism or damage from external sources such as debris and wildlife, which could compromise the pressure in the system. Therefore, security would be necessary for guarding the safety of the overground tunnel. In contrast, an underground Hyperloop system would be less exposed to these factors, however, maintaining an underground system comes with more challenges such as the geology and topography of the area it travels through. Although the underground scenario may require less maintenance and repair due to less exposure, access to the tunnel poses difficulty and will be time-consuming whilst above ground may need constant repair it will be easier to access. [6]

Conclusion

To conclude, the overground scenario seems like the best option of the two, from an environmental, economic, and technical standpoint. The overground tunnel has a higher risk, and the upkeep and protection against risk are easier and cheaper making this justifiable from an economic standpoint. Risk is more easily mitigated again for the overground whereas the underground is limited to modification. Although, underground poses less disruption in various areas such as construction, wildlife, environment, it is very expensive not only to construct but upkeep making it become inundated very quickly posing the risk of catastrophic failure sooner. Therefore, the overground seems the more likely scenario as not only this can probably be afforded and constructed, but there are grounds for mitigation which improve the safety of the passengers.

4.2. The Kantrowitz Limit

With its ability to travel at incredibly high speeds, Hyperloop introduces a number of unique conditions that require careful consideration that are not taken into account in other modes of travel. The pod and the tunnel have a similar diameter, so as the pod travels through the tunnel at high speed, the tunnel creates a restraint for air to pass the vehicle and restricts airflow. This results in a pressure build up at the front of the pod which is created by the trapped air which cannot pass. This in turn increases the drag on the pod and limits its speed [1]. This effect is called the piston effect which has other implications such as a sonic boom or tunnel boom which can create a loud sound, effect aerodynamic performance and damage the strength and structural integrity of the tunnel.

The Kantrowitz limit is a sonic condition which determines the stalling condition of gas flow at transonic speeds flowing through a narrow path and is the maximum amount of compression before the flow chokes [2]. Once the Kantrowitz limit is reached the and the flow is choked and the pod begins to behave as a piston which increases the adverse pressure against the pod, increasing the drag and increasing the power required to propel the pod. Therefore, ways to mitigate choked flow and the Kantrowitz limit are required to prevent a detrimental effect on the performance of the system [3].

One way to mitigate the effects is by using a compressor on the pod or within the tunnel walls, which is predicted to reduce the drag if the pod is operating above the Kantrowitz limit. Using a compressor almost always reduces the power consumption of the pod if operating over the Kantrowitz limit and can have a maximum power reduction of up to 47.5% [3]. Despite this, the compressor only increases power consumption above the Kantrowitz limit and can be a very expensive addition to the system.

Another method is the attachment of airfoils to the pod, which when modelled using computational fluid dynamics techniques, shows a Kantrowitz limit of 1.07 times the model without airfoils, suggesting that the model without airfoils chokes the air earlier than the airfoil model. Therefore, the addition of airfoil fins to the shell of the pod is a feasible

technique to mitigate drag and the piston effect, although it involves a redesigned shell for the pod [1].

In the following report, these effects are mitigated by having the pod operate under vacuum, the conditions and associated requirements are discussed in the following sections.

4.3. Tunnel Materials Selection

4.3.1. Ductile-to-Brittle Transition

Creating a high vacuum in a tunnel carries with it possible risks and, by extension, concerns for us as engineers. The first concern to discuss is the relationship between a material's mechanical properties and its temperature. The ductile to brittle transition temperature (DBT) is the primary concern in this case. When a ductile material such as a metal alloy cools below this threshold, it exhibits brittle fracture behaviour and therefore will have poorer mechanical properties than predicted when designing a component. This can lead to unforeseen damage within the component, and possibly even catastrophic failure.
In this case, depressurising a vessel leads to an associated temperature drop as can be determined by the Ideal Gas Law, pV = nRT. The risk of the internal temperature of the tunnel dropping below the DBT of HSLA prompted our research into this topic.

Our calculations have found that the temperature isn't predicted to drop below 0ºC. (see 4.4.1.3.). Fortunately, HSLA steel's DBT is dependent on strain rate, and G. H. Mazjoobi et al's research found that at -40ºC, no transition was observed across several strain rates [6]. This further reinforces how HSLA steels are an optimal choice for this application.

4.3.2. Vacuum Buckling

Vacuum buckling describes the inward collapse of the tunnel due to external pressure exerted due reduced pressure inside the tunnel [1]. If the tunnel material is too weak or not thick enough, it is susceptible to collapse. Since high vacuum conditions inside the tunnel is a requirement in Hyperloop design, vacuum buckling is a risk that must be accounted for but can be mitigated against by designing a tunnel with high strength and appropriate thickness. Therefore, tunnel material selection and dimensions are critical when discussing the full-scale technical integration of an Hyperloop pod.

Nuclear fuel tunnels for example experience around 15.5 MPa of external for due to the pressurised water reactor [1]. This is also a risk accounted for in the food and pharmaceutical industries, as large vessels that are discharged of their contents rapidly are at risk of vacuum collapse [2]. In these industries integrated support structures and pressure control systems are used to ensure they components operate within a safe range [2].

Mechanical properties of a material such as its Young's modulus and Poisson's ratio (both of which critical pressure is dependent on exist with a level of uncertainty and are not constant between different samples of the sample material. In addition, irregularities in the tunnel shape also will lead to the calculated critical pressure value having a degree of uncertainty [1]. To account for this uncertainty, the ideal operating range for the materials must be well below

its yield stress to minimise the risk of failure, as well as dimension tolerances when considering tunnel thickness and radius.
Pressure vessels are typically designed with a safety factor ranging between 3.5-6 [3]. This system will be designed according to a safety factor of 4.

To calculate the critical buckling pressure (ρ_{cr}) of a cylindrical tube

$$\rho_{cr} = \frac{0.25E}{1-\nu^2}\left(\frac{t}{R}\right)^3 [4]$$

Such that t = wall thickness and, R = tunnel radius, E = Young's modulus of the tunnel materials, and ν = Poisson's ratio of the tunnel material. Therefore, the critical buckling pressure is dependent on but the material and its conditions. Note that ρ_{cr} refers to the external pressure acting on the vacuum tunnel – 100 times atmosphere in this case.

As discussed, we propose that high strength low alloy steel be used to construct the tunnel. HSLA steels have a Young's modulus, E of at least 183 GPa [5] (See AP B.1), and a Poisson's ration, ν of up to 0.300 [5] (See AP B.1). Assuming a tunnel radius of 1.5 m, with a target external tunnel pressure, ρ = 10.1325 MPa, the minimum tunnel thickness required for a safety factor of 4 is **13.96 cm** (See AP B.2). This equation assumes a perfectly cylindrical, infinite tube with no joins, therefore, in practice, the tunnel with have to be thicker to compensate for weaknesses along the tunnel such as welds.

4.3.3. Tunnel Design

Materials selection of the tunnel – corrosion resistance and thermal expansion
Our approach to designing tunnel structure was initially to consider reactor pressure vessel design. These are designed in the interest of operating extreme pressure environments and maintaining corrosion resistance in high-temperature, corrosive environments.

One approach that was considered was modelled on the Davis-Besse reactor pressure vessel for example is a high strength low alloy (HSLA) steel vessel with a stainless steel internal cladding [1]. HSLA steels have poor corrosion resistance as iron is a strongly anodic and reactive metal [2][3], leading to its high susceptibility to corrosion. In addition, low concentration of alloying elements in the steel meaning the iron has little corrosion protection [4]. Stainless steel however is comparatively lower strength and would not be appropriate for such an application [5] but does have a greater corrosion resistance than HLSA steels due to the passivity provided by alloying elements, chromium specifically [3]. This approach would facilitate a high strength tunnel with protection from environmental corrosion [4].

Conditions inside a Hyperloop tunnel however are not as extreme as those in reactor pressure vessels (RPVs) such as Davis-Besse. Neither the internal nor external environments are as electrochemically aggressive as those in an RPV. Therefore, corrosion protection such as stainless steel cladding, although effective, would incur additional costs that aren't necessary. A more cost-effective approach would be applying a polymeric barrier coating [6].

The polymers used and the thickness of this barrier coating is specific to the corrosion rate of the steel in its environment [6]. Other design parameters that must be considered are the lifetime and ease of application and repair of the polymer coating, as well as its thermal conductivity.

An above ground tunnel will by experience temperature fluctuations during service that need to be accounted for. Weathering poses the threat of not only corrosion of the tunnel but thermal expansion. On a scale as large as an Hyperloop tunnel, slight fluctuations in tunnel size can cause significant damage to its infrastructure. Therefore, designing a tunnel with a low thermal expansion and/or thermal insulation is critical.

Polymeric foams are commonly used as insulation. While resistant to thermal conduction, the porosity of a polymer foam would not aid in providing corrosion resistance. A non-porous polymer coating, however, will provide both insulation and corrosion resistance. (See AP A.1).

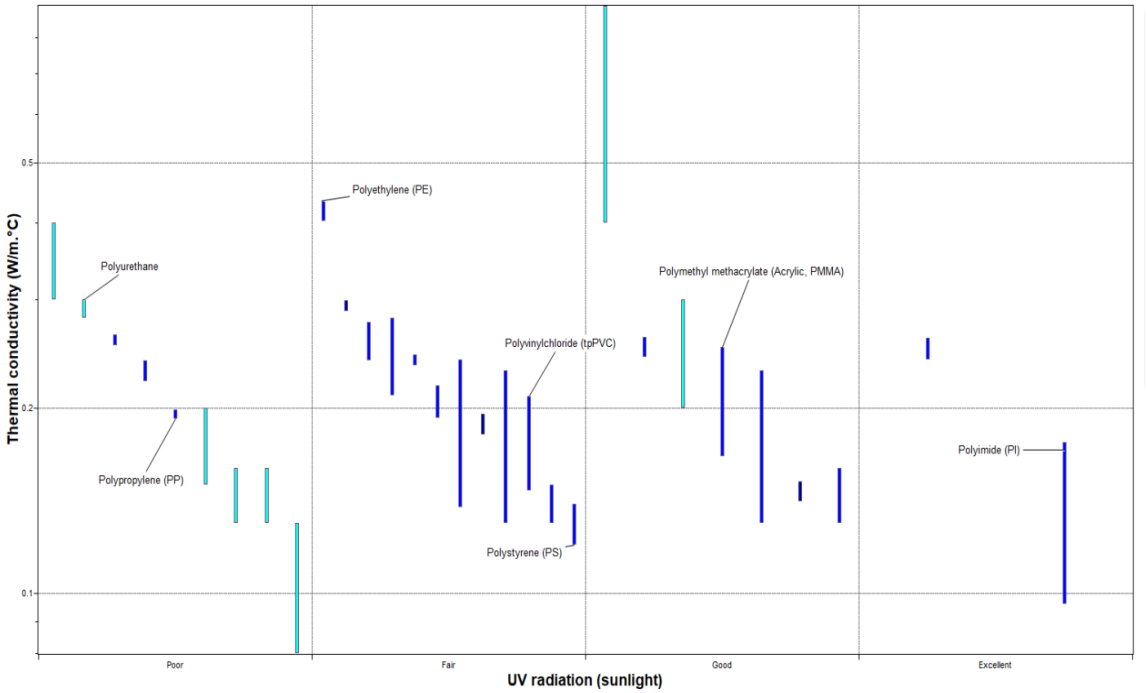

Figure 1: Ashby plot comparing thermal conductivity of various polymers with respect to their resistance to UV radiation (sunlight). (See AP A.2)

An Ashby plot comparing various polymers' resistance against UV radiation with respect to their thermal conductivity (fig. 1) allows us to compare their abilities to insulate the Hyperloop tunnel against the longevity of their usage before degrading in the outdoors.
As is clear in the figure above, while PVC for example has a relatively low thermal conductivity (~0.15-0.22 W/mºC), its resistance to UV exposure is 'fair'. Polyimide (PI) however, has both a low thermal conductivity coefficient (~ 0.09-0.18 W/mºC) and an 'excellent' resistance to UV radiation. Polyimide is used in medical tubing due to its chemical resistance [7], therefore it can provide appropriate corrosion resistance and will last long enough to make maintenance over time more affordable – an important characteristic when designing infrastructure. Therefore, a polyimide protective coating was selected to insulate the tunnel and prevent environmental degradation. (See AP A.3).

Materials selection of the tunnel – the tube itself

Encasing a train that runs above ground is a novel approach, as currently trains are designed to travel through atmosphere. Underground tunnels are reinforced using high-density concrete that limits ground-borne vibrations and overcomes hydrostatic pressure [8]. Although effective, this application cannot be directly translated to an above ground approach. In order to support a high-density tunnel above ground, the supports must be able to bear a much higher load than may be necessary. An additional concern would the integrity of the land itself, and whether it could withstand a high load without sinking and causing structural damage to the tunnel over time [9](see 4.1).

Therefore, comparatively less dense metals have been considered as options when selecting tunnel material.

The factors being considered are stiffness and fatigue strength with respect to cost.

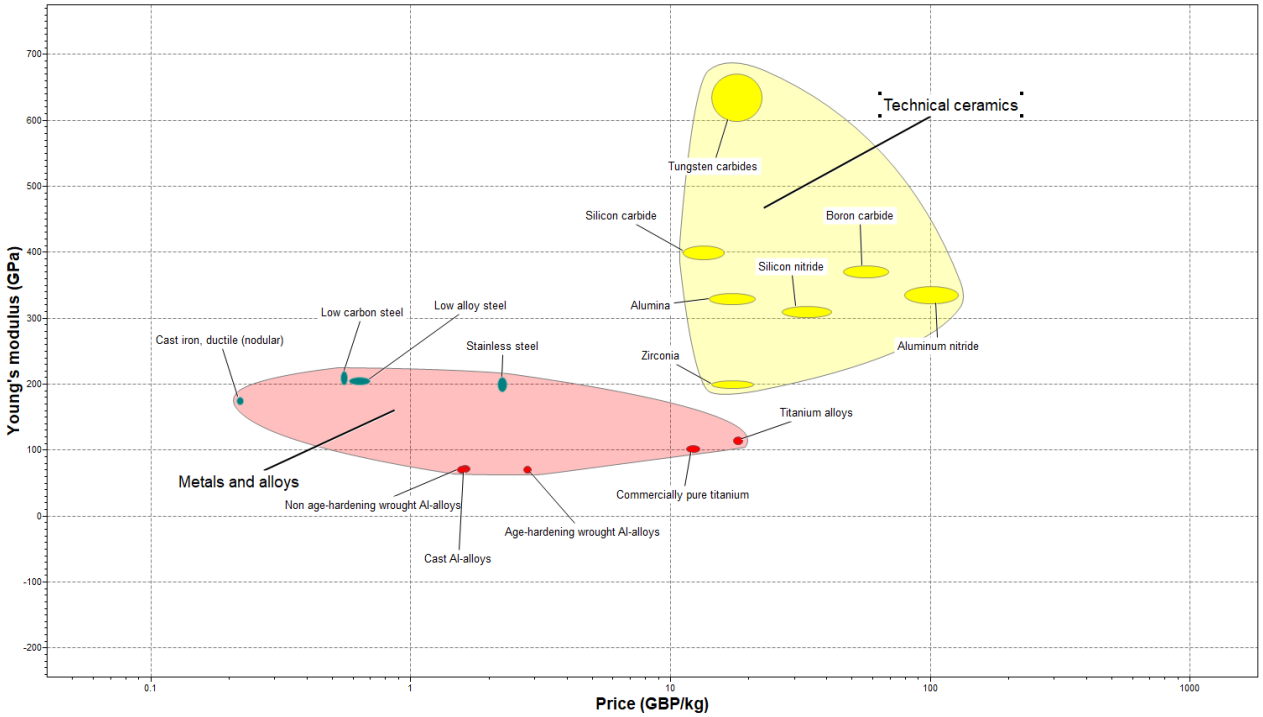

Figure 2: Ashby plots comparing the Young's moduli (stiffness] of various engineering alloys and ceramics with respect to their cost per kilogram .(See APA.4)

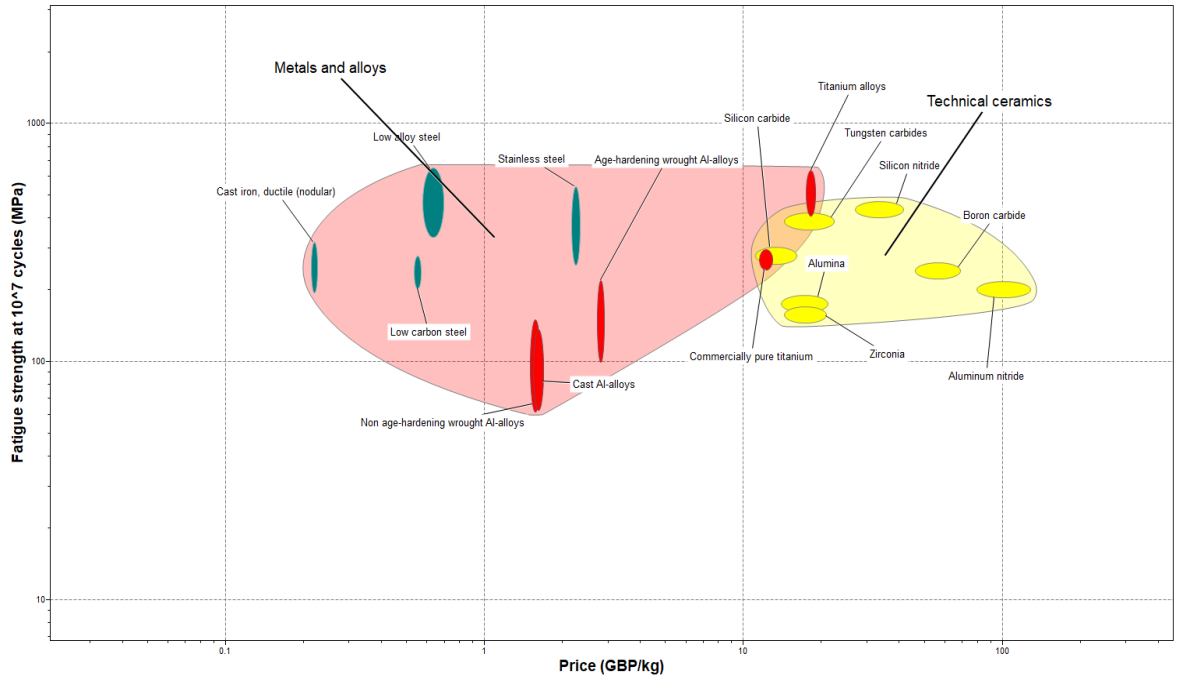

Figure 3: Ashby plot comparing the fatigue strengths of various engineering alloys and ceramics with respect to their cost per kilogram. (See AP A.5)

As expected, considering their common industrial uses, steels are both cheap and stiff compared to other alloys and technical ceramics as evident in figure 2. The same is true for their fatigue strength, (fig 3.) with superior properties to Al-alloys and technical ceramics.
As discussed and re-iterated by figures 2 & 3, HSLA steel are an appropriate selection for tunnel material – both low cost and high strength compared to other metals, alloys, and technical ceramics. What remains is to consider mechanical constraints the tunnel while in use, and account for them in our design.

4.4. Inducing and Maintaining a Vacuum

4.4.1 Rotary Vane Pumps

4.4.1.1 Working Principles of Rotary Vane Pump

Using the electromagnetic forces of magnets adjusted in a specific direction and at a certain distance will generate movement. Carefully designing the angles of each magnet towards the other will enable rotation around the centre rod. This is connected directly to a helix shaped propeller within a chamber. This chamber is where the low point pressure is obtained, due to the shape of the rotor plate in the pump. This low-pressure point when connected to an air-filled volume, pulls the air in its direction to reach an equilibrium. As the plate turns quickly, that air is trapped and evacuated through the evacuation chamber. Then a new pressure point is created, and more air is sucked out which little by little enables it to reach a certain vacuum level.
The time it takes to reach a near-vacuum state will depend on how low the low-pressure point is. In an ideal case, after some time the pressure in the tube will get closer and closer to the low-pressure point. The flow rate of evacuated air, or emptying rate, behaves exponentially

with respect to time, due to the constantly reducing pressure of the volume that is being evacuated. Therefore, we need to find an ideal point where the vacuum friction is negligible, while the vacuuming is time efficient. A detailed set of illustrations for this system can be found in AP C.1 [4].

4.4.1.2. The pressure valve system

There must exist a valve within the vacuum pump system to prevent back flow of air being evacuated or having already been evacuated by the pump. If not, air will flow back from the ambient atmosphere to equalize the pressure differential generated by the vacuum pump. A tap-based valve will be implemented to allow air flow in one direction and prevent any flow in the other. The focus should be its mechanical simplicity to prevent it being a point of failure for an already complicated system as is. This following diagram from Tameson illustrates this concept.

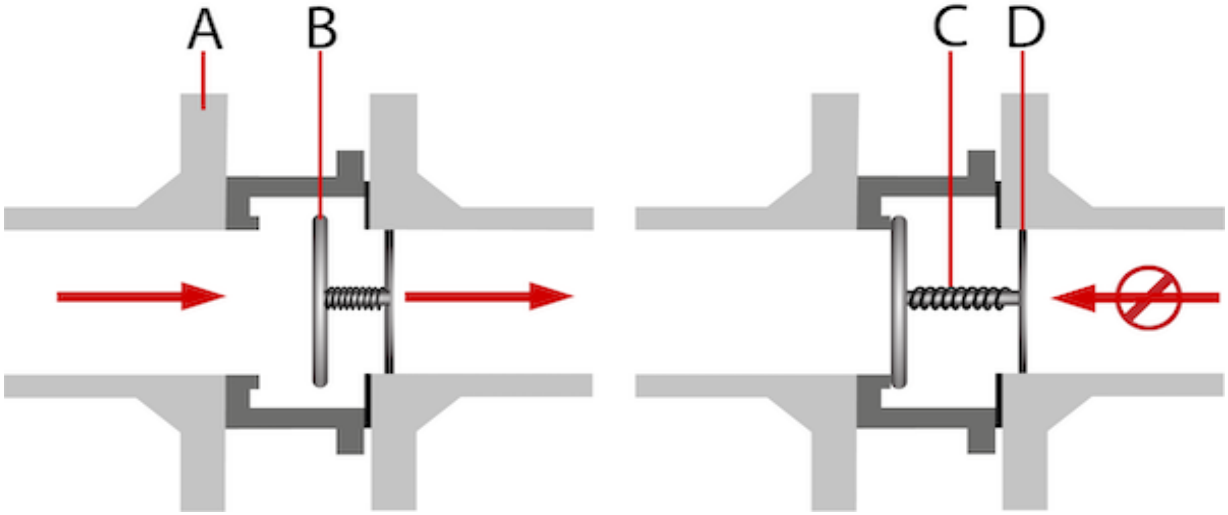

Figure 4: Generic pressure valve system [6]

4.4.1.3 Vacuum pumping formulae and graph behaviour

This system must be analyses from a fundamental engineering perspective, thus, it is necessary to make assumptions about boundary conditions of this system and how the elements of its control volume behave. First, the bounding box for the control volume itself should be concretely set up. The control volume for this system encompasses the volume of air within any set length of the Hyperloop tunnel, and the pathway which leads the valve and pump for said section of the tube.

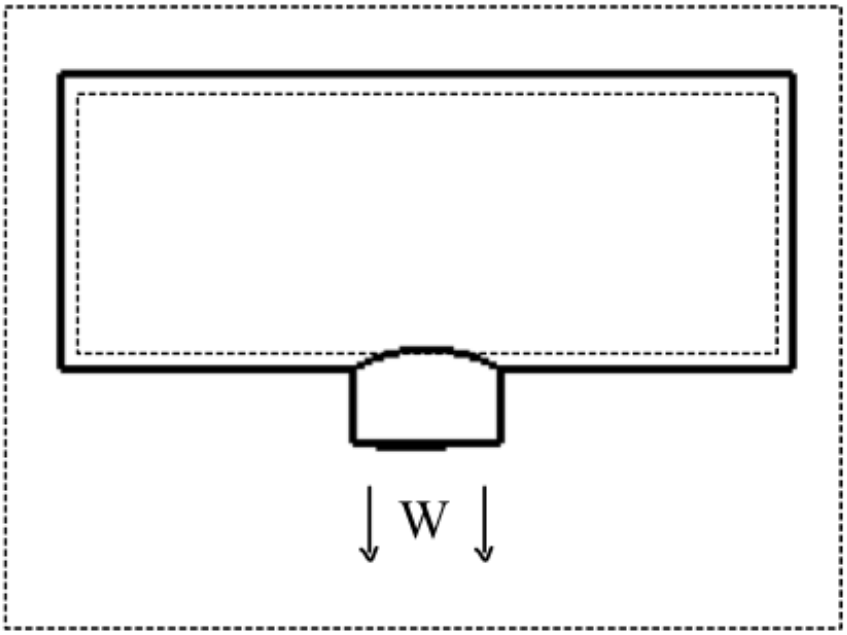

Figure 5: Control Volume (CV) considered in vacuuming a tube.

Secondly, we assume that the ambient pressure within the tube is identical to the exterior ambient pressure, hence neglecting effects of condensation due to temperature variations. This assumption is founded on the choice of taking the control volume as adiabatic. Though heat transfer by radiation will occur gradually from the ambient surroundings into the control volume as the tube will be constructed of a metal alloy. However, we decided that the rate of this occurrence would be incredibly low and can be neglected especially during the pumping phase.
Thirdly, no losses occur in the control volume. No ambient air makes it into the control volume during standard operation. The case for purposely depressurizing the system is made separately. No losses are assumed to occur passively in the tube or the vacuum system.

Though the pump is “pumping” air out of the CV, it is flowing out to equalize the pressure drop. Therefore, it is like emptying a bike tire, with respect to the exterior (low pressure point in the pump), the tank is pressurized. When discussing this system, it is essential to point out that volumetric pumping rates do not apply here. Indeed, it is the volume that is constant and the pressure that reduces. This makes estimating pumping times overly complex. Similarly, to a reactor jet, with less air density, efficiency reduces. However, pressure in a constant volume does not reduce linearly, instead it follows an exponential attenuation. The following graph example will further illustrate the purpose. From a behavioural point of view, what affects the curve are: the starting pressure, the volume, and the pumping speed which is specific to the pump but can be considered as a performance index.

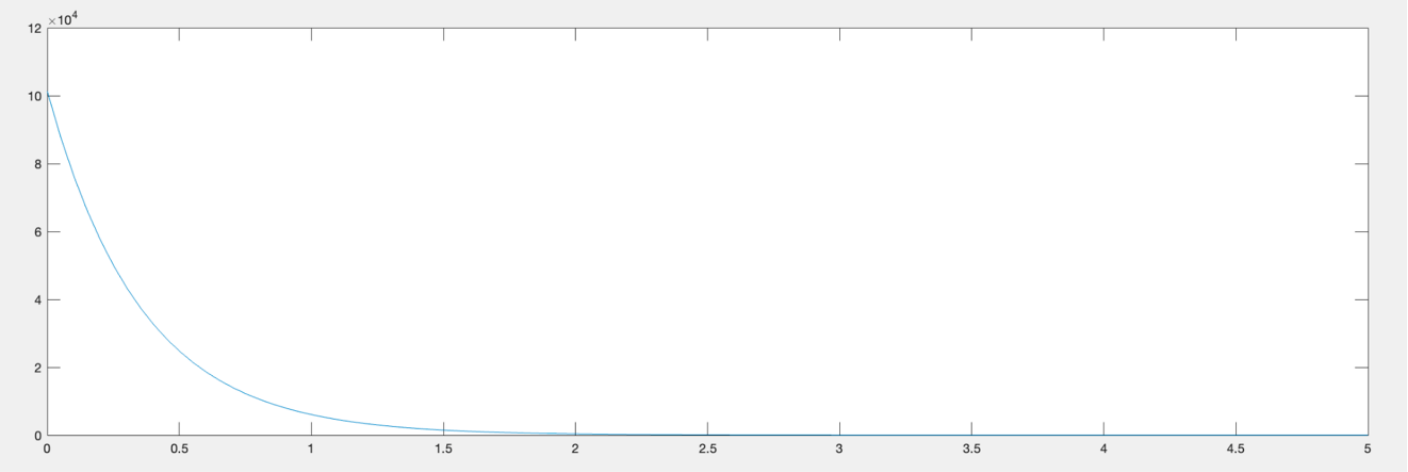

Figure 6: Air Pressure reduction as a function of time for generic pump.

After considering the drag energy induced to the pod by air, and the pressure reduction through time while vacuuming, it was deducted that 1% atmospheric pressure, or 1013.25 Pa is the ideal fit.

This was achieved by employing fluid dynamics and plotting graphs for the formulae outlined below. As much as it would be ideal to aim for a higher value in order to decrease air resistance further and improve the efficiency of energy used in propelling the pod, it was discovered that it would result in diminishing returns for the amount of energy and effort required to generate a high vacuum and maintain it, not to mention the higher risk of mechanical failure due to more pumps and more moving parts required to run the system. This will be further expanded upon later on in this paper.

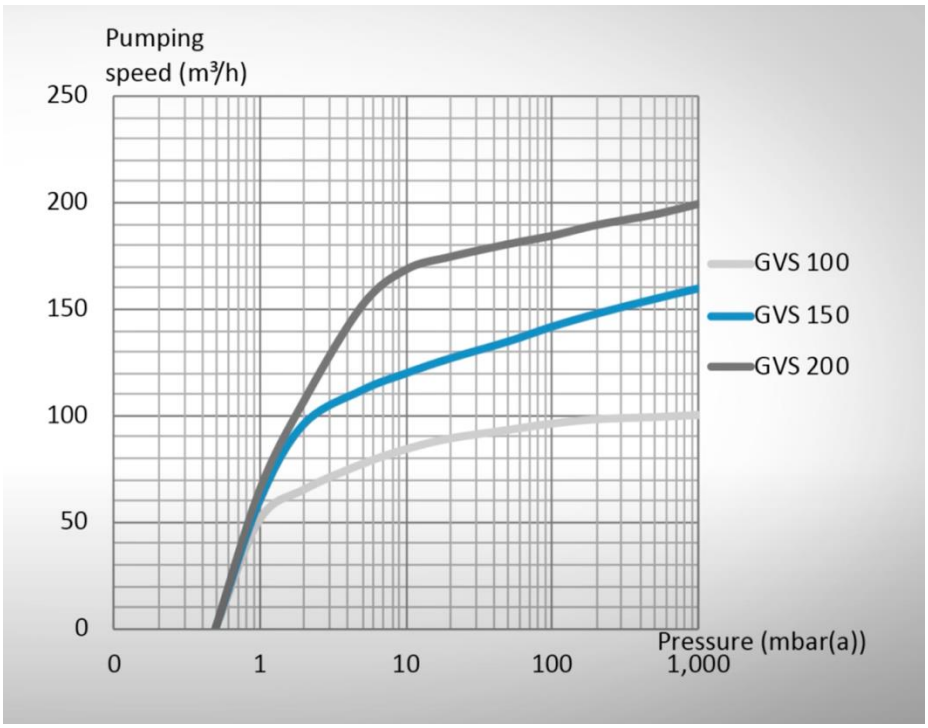

Figure 7: Pumping speed at various pressures if constant for generic pump (See AP C.2)

Here, from one bar to 1 mbar, pumping speed reduces by 20 percent in the worst case therefore we can either average out the change or just neglect it. In this case, we chose to reduce the pumping speed of 10% of its first performance to 1 bar and take it as continuous through the pumping process.

The following formula traces “de-pressurization” as a function of time;
Given that

$$P(t) = P0 * \exp\left(t * \frac{S}{V}\right)$$

Which transforms into a natural log function when calculating the pump down time.
Pump down time: $t = \frac{V}{S} * \ln\left(\frac{P0}{P1}\right)$

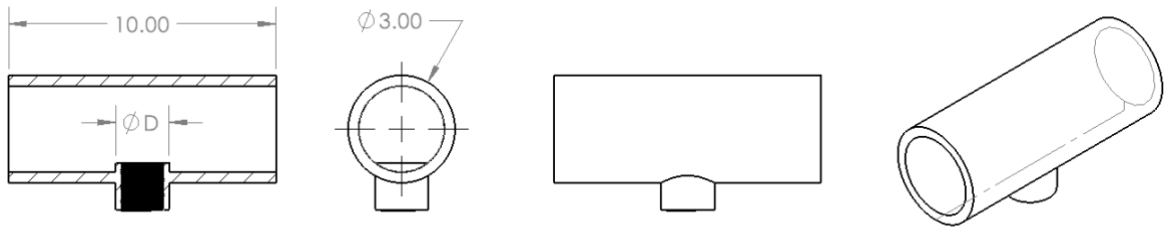

Figure 8: Tube dimensions on Solid works.

Using our data for the tank we can estimate our volume, we already have initial and final pressures, and the pumping speed is taken as a reasonable generic pumping speed.

P1 is 1 atm or 101325 Pa
P2 is 0.01 atm or 1013.25 Pa
V-tank=71 m^3 (about the volume of a one car garage)
Pumping speed S $\sim 220m3/h$
Adjusted pumping speed S$\sim 200m^3/h$
Calculating an estimated pumping time to reach 1% vacuum, i.e.,1013 Pa

$$T = \frac{71}{200} * \ln\left(\frac{101325}{1013.25}\right) = 1.6h$$

4.4.1.4 Market Options & Comparison

Below are presented three suppliers with convenient products with respect to our need.
Becker; U 5.201; ROTARY VANE VACUUM PUMPS, OIL-LUBRICATED 1]
Specs:
S=$200m^3/h$
P of convergence = 0.1 mbar
Weight = 70 kg

Pros: Integrated non-return valve
Oil Less system, better maintenance
Cons: Pricing not displayed

"Madeinchina;" 5.5kw; $200m^3/h$ Rotary Vane Vacuum Pumps [2]
Specs:
S=$200m^3/h$
P of convergence = 0.1 mbar
Weight = 140 kg
Pros: Large supplier
Cons: Shipping cost and lack of visibility

Woosung vacuum Pumps; MPV240 [3]
Specs:
S=240 m^3/h
P of convergence = 5*10-4 bar
Weight = 200 kg
Pros: Integrated Valve system
Cons: Shipping cost and lack of visibility

Comparing these suppliers, one sticks out both for practicality and performance, indeed Becker as a UK based supplier will enable simpler and straight forward service. It also supplies an integrated valve as part of the package which further simplifies the process, removing the Hussle of ensuring proper compatibility between pump and valve suppliers. Reviews are positive and underline this pump as a cheap effective system.

4.4.2 Novel Design Approach

Concerning our Hyperloop system, we are aiming to achieve a 1% atm vacuum, which corresponds to 10.1325 mbar. This can be identified as a low or rough vacuum (LV). We then have to find a suitable pumping mechanism for our vacuum condition. The operating ranges of major pumps are shown in the chart below with an indication of the order of magnitude of speed. [1]

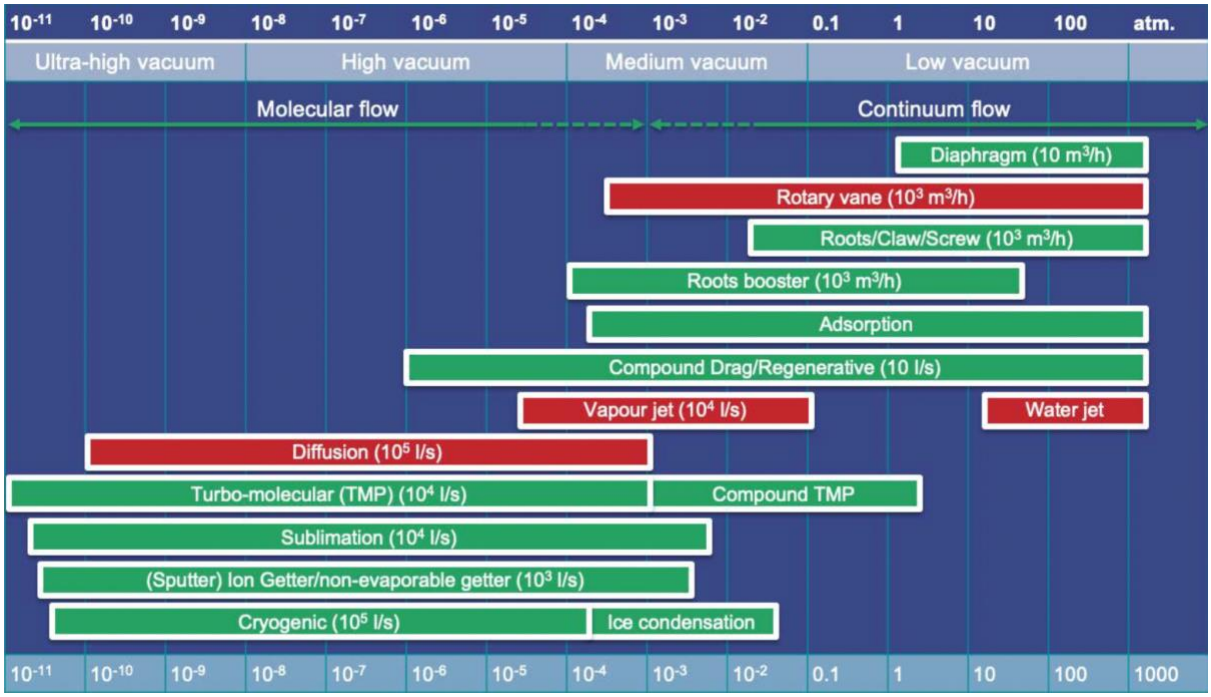

Figure 9: chart of the different types of vacuum pumps [1] Green represents dry and red represents oil/fluid mechanisms.

Considering figure 9, we can establish a first list of 7 pump types that can produce a low or rough vacuum.

Design of the pumping system

After investigating these different pumping systems, we realised that it was perhaps wiser to take inspiration from one of them in order to be able to develop a new one precisely adapted to our case. Of all of these pump types, the vapor jet pump seemed to have some convenient characteristics. Indeed, there is no moving part in the pump, only flows of fluids, and its use seems much more appropriate than other pumps without moving parts such as adsorption pumps for example. With a vapor jet pump, the air that is absorbed from the tube would be mixed with the high-speed stream of vapor. To simplify this situation, we would like to replace this fluid with air. This way the mixture keeps the same composition.

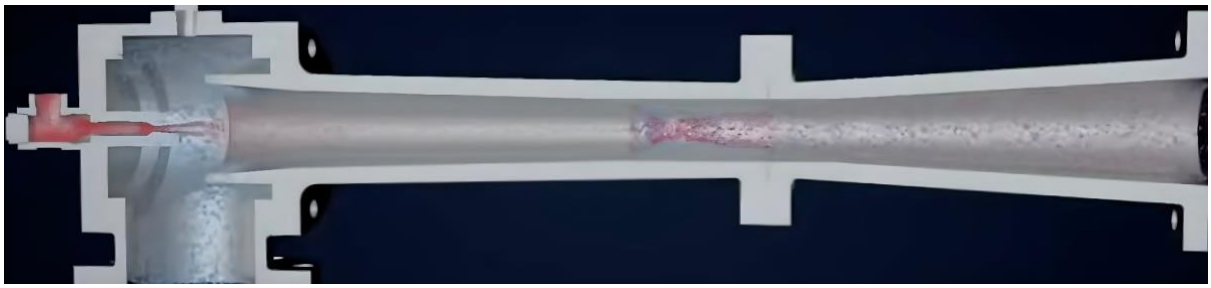

Figure 10: Stream jet ejector [2]

To create a very efficient system we would like to place venturi tubes in series so that the pumping process can take place along the whole tube continuously. The pumping system would be located below the tunnel with several connections placed at constant intervals between the tunnel and the venturi tubes. We decided to place a compressor at the inlet of

the system to create a high pressure before the flow enters the small convergent-divergent (C-D) nozzle. The flow is supposed to be supersonic at its outlet. In that case, an increase in the cross-sectional area would lead to a decrease in pressure and an increase in velocity. The high velocity generated should then produce the desired suction through the tunnel connection. The created mixture would pass through the big C-D nozzle and exit it at a subsonic velocity, leading to higher pressure and lower velocity as the cross-section increase. The high pressure generated would enable us to connect another small C-D nozzle similar to the first one and repeat the previously described process.

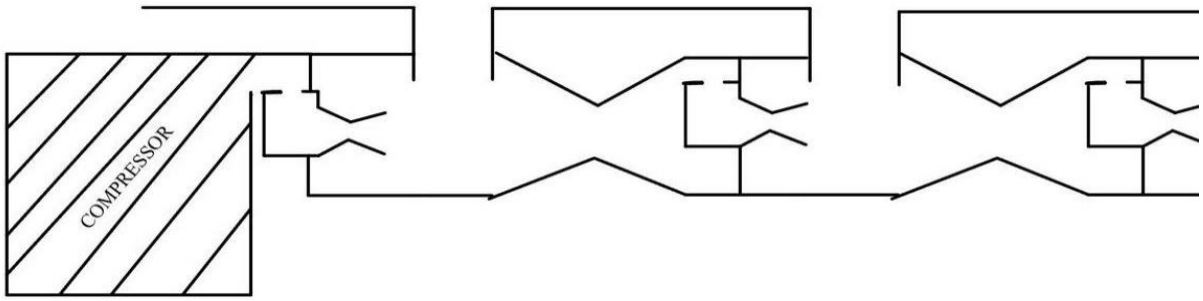

Figure 11: Sketch of the venturi tubes pumping system.

Of course, uncontrollable losses will occur in service (such as frictions, and thermal inconsistencies). It is therefore necessary to use another compressor along the system, from a distance to the previous one where the losses become too important.

Design of a throat with a variable cross-sectional area

Using isentropic relations, it is possible to express the exit pressure of the nozzle as a function of the area ratio and the inlet total pressure. We can see from the graph below that for a fixed total inlet pressure, as the area ratio increases, the exit pressure of the flow also decreases accordingly.

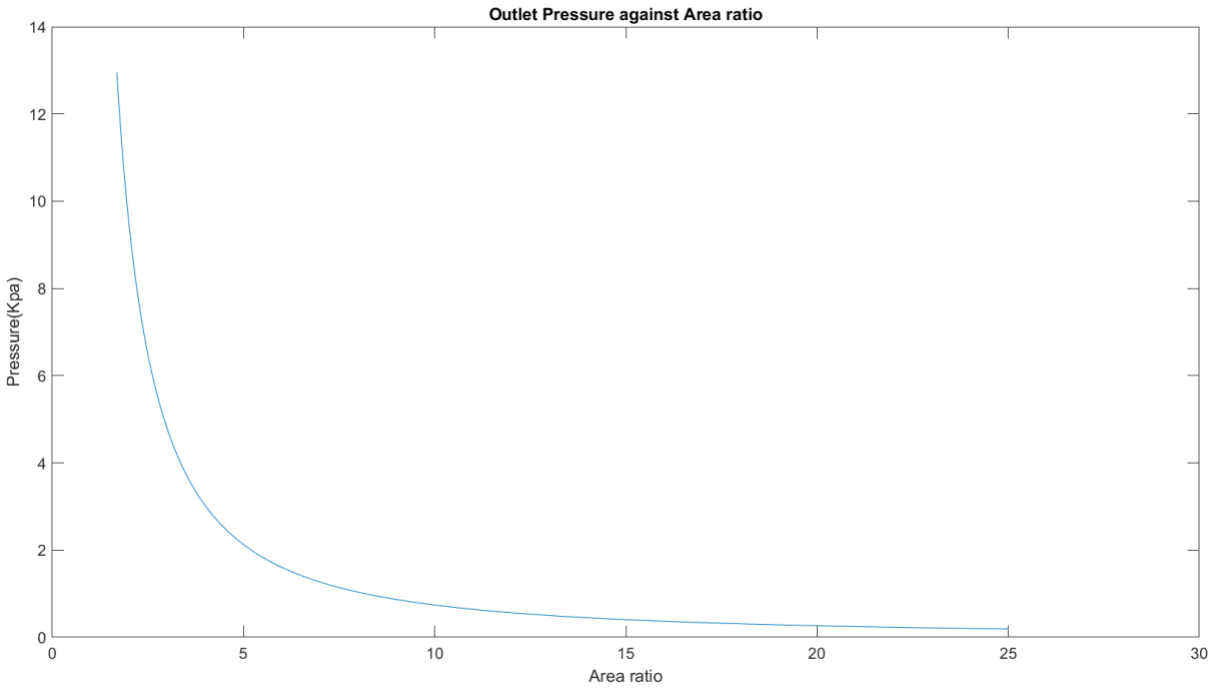

Figure 12: The outlet pressure as a function of area ratio

Gradually increasing the area ratio therefore reduces the exit pressure in the diverging section. Thus, we investigated a suitable solution for varying the cross-sectional area of the throat. Our first design concept was inspired by the exhaust of a jet engine.

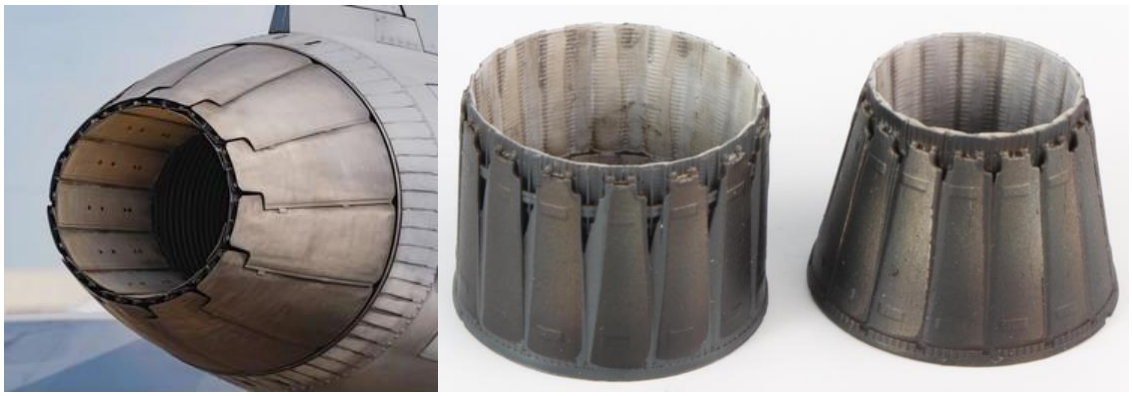

Figure 13: Jet fighter, jet engine exhaustion and F100-PW-200 exhaust nozzle [3]

As can be seen in the previous photos, the fighter jet exhaust system allows the area to be varied. We therefore wanted to use two similar nozzles facing each other at the throat of the C-D nozzle of our system. However, this device is quite elaborate and contains many moving parts. For this reason, we decided to investigate further and find a simpler way to solve our problem. The idea of using a part similar to a spindle then emerged. The spindle would become increasingly sharp and moving it along the x-axis through the throat would allow the area of the cross-section to vary.

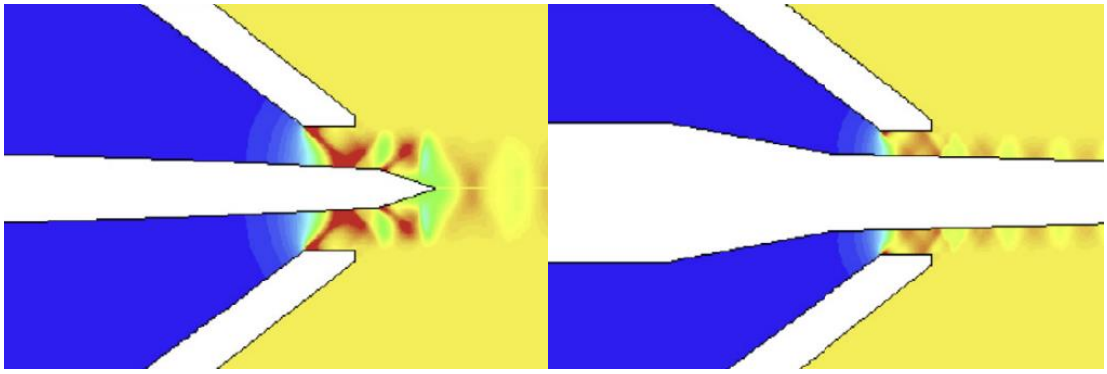

Figure 14: Spindle at 95% compared to spindle at 10% (left to right) [4]

Compared to the first design, this one has only one moving part, is much easier to use and the maintenance needs are drastically reduced.

Final operating design conditions

In order to demonstrate the ideas behind the system, we will do the analysis of two successive convergent-divergent nozzles. We will determine the pressure, temperature and velocities required at the inlet and outlet of each convergent-divergent nozzle using hand calculations and matlab. The following calculations solely intend to demonstrate the feasibility of the project because in real life, these parameters will be automatically controlled using a feedback control system.

FIRST STAGE (FLOW THROUGH FIRST C-D NOZZLE)

At a final pressure of 1% atm, the outlet temperature was chosen to be 240 K. Using the ideal gas law equation $Pe = \rho \times R \times T$, the density of the flow is found to be $\boldsymbol{\rho e} = \mathbf{1.47 * 10^{-5}}\ kg/m^3$

We want to operate in a cycle, which means that after the first supersonic transition, we want to be able to recompress the flow and redirect it into another convergent divergent nozzle. This is solely done by using an appropriate geometry in the nozzle. However, since the pressure at the outlet of nozzles will be as low as 1%, and the density of the primary fluid significantly reduced, the flow will need to have a considerably high velocity in order to have enough momentum and push against the upstream built-up pressure. This means that at fixed conditions, there is a maximum recompression threshold that the flow should stay under.

Using the momentum equation, it can be deduced that the change in pressure across the nozzle is $dp = -\rho u du$, with $du = ur - ue$, and $dp = Pr - Pe$. We want to be able to find the maximum pressure Pr that will bring the flow to rest(e.i: $ue = 0m/s$).

$$dp = \rho u du \ \leftrightarrow\ Pr - Pe = -\rho ue\ (ur - ue)$$

By putting $ue = 0$, we can find that the maximum recompression pressure (Pr) allowed is equal to **$\rho(Ue)^2$+ Pe.** This tells us that the threshold pressure depends on the outlet flow

velocity and density, and that the maximum pressure increases with the outlet velocity of the convergent-divergent nozzle. For a fixed recompression pressure desired, the minimum velocity of the flow needed can therefore be expressed as following:

$$\boldsymbol{Pr = \rho e * Ue^2 + Pe \;\leftrightarrow\; Ue = \sqrt{\frac{Pr - Pe}{\rho}}}$$

At the same time however, this build up pressure will have to be great enough to directly produce supersonic flow in the following nozzle, as we do not want the occurrence of shock wave resulting from subsonic-supersonic transition. This means that the threshold pressure itself has to be greater or equal to 1 atm (101325 Pa), as we need to be able to compress the flow back to this pressure in order to produce a fully supersonic flow in the divergent section.

By fixing Pr (Recompression Pressure) at 1 atm (101325 Pa), we can find that our flow will need to have a speed of at least 2611 m/s in order to have enough momentum to keep moving. This is further illustrated by the figure 15.

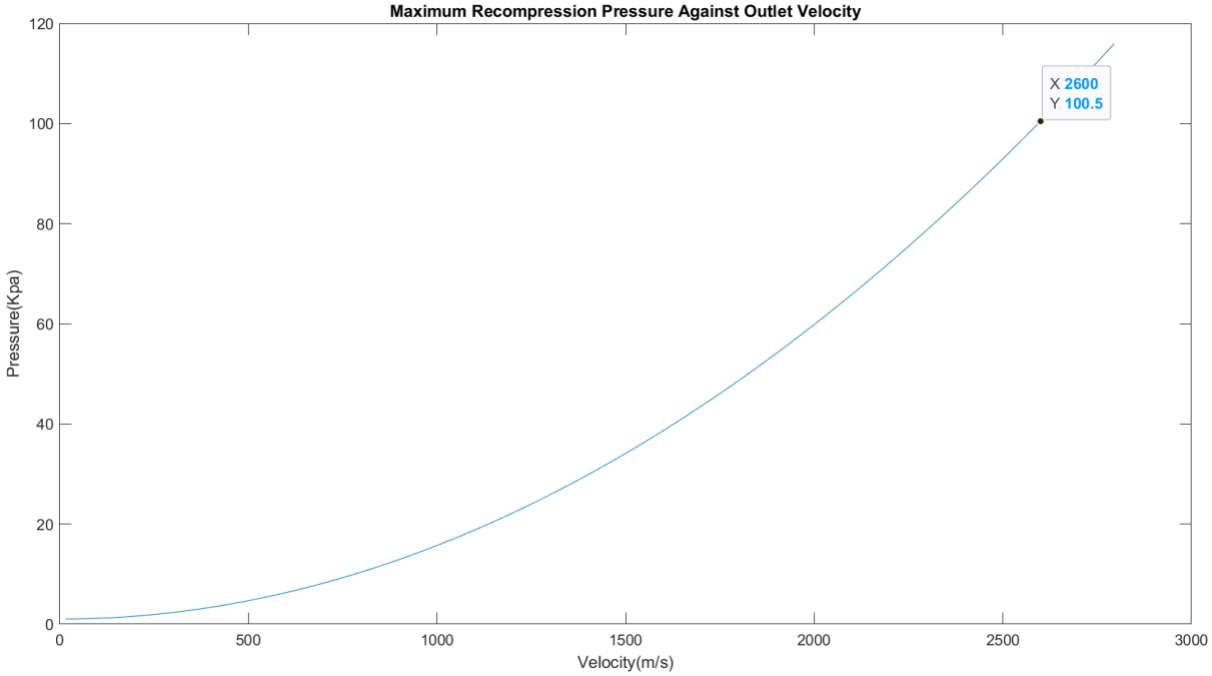

Figure 15: Maximum recompression pressure as a function of outlet velocity

Knowing the required speed and the temperature, we can therefore find the Mach number of the flow using $Me = \frac{Ve}{\sqrt{\gamma RTe}}$. For Ve =2611m/s and $Te = 240K$, we can determine Me to be equal to 8.41, as seen in the figure 16.

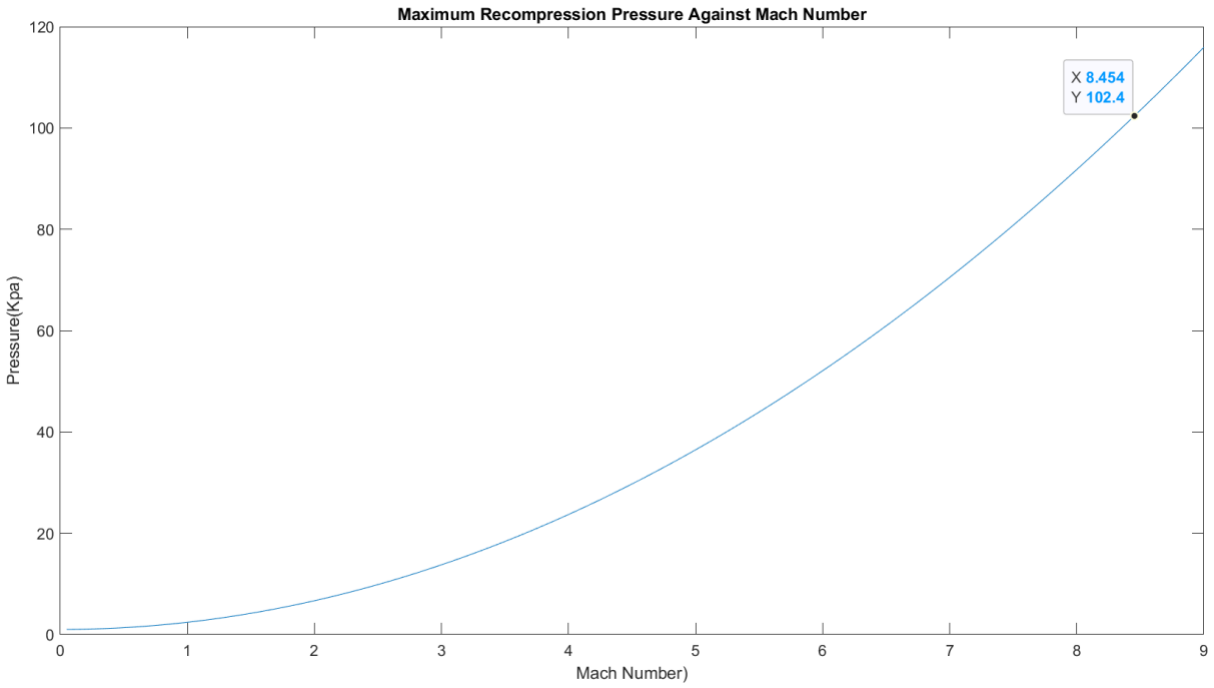

Figure 16: Maximum recompression pressure as a function of Mach number

Knowing the Mach number at the outlet, we can therefore determine the final area ratio and the inlet total pressure required at final operating conditions.

From the isentropic table we can see that at a Mach number of 8.41,

$$\frac{\mathrm{Po}}{\mathrm{Pe}} \simeq 15341.5 \leftrightarrow \ \mathrm{Po1} = 15431.5 * 1013.25 \ \leftrightarrow \mathrm{Po1} = 15.64\mathrm{Mpa}$$

Assuming air is an ideal gas, we can calculate the temperature of the air at a pressure of 15.64 MPa starting from atmospheric conditions (an initial temperature of 298 K (25°C) and pressure of 101325 Pa) using the following equation:

$$\frac{T2}{T1} = \left(\frac{P2}{P1}\right)^{\frac{\gamma-1}{\gamma}} \ \leftrightarrow \ T2 \ = 1257.5\ K$$

Therefore, the pressure of the air after going through the compressor will have to be at least 15.64 MPa, which will correspond to a temperature of 643.6K. By varying the cross-sectional area, we can then obtain a pressure of 1% atm at the exit. The final area ratio at these operating conditions will be approximately equal to 258.65.

SECOND STAGE (FLOW THROUGH SECOND C-D NOZZLE)

Following the first re-compression, the flow is then ready to go back into the following convergent-divergent nozzle. The pressure reached after the first re-compression stage is greater or equal to 1 atm, so we can produce a supersonic flow in the second nozzle by varying the cross-sectional area, as discussed earlier.

The first re-compression pressure corresponds to the total pressure at the inlet of the second convergent divergent nozzle. Knowing that the pressure at the exit of the first nozzle is 1% atm (Pe=1013.25Pa) and the temperature 240K, we can determine the temperature reached by the flow when it gets re-compressed up to Pr = $\mathrm{Po2}$ = 101325 Pa.

$$\frac{\mathrm{Tr}}{\mathrm{Te}} = \left(\frac{\mathrm{Pr}}{\mathrm{Pe}}\right)^{\frac{\gamma-1}{\gamma}} \leftrightarrow \mathrm{Tr} = 894.622\ \mathrm{K}.$$

With an inlet total pressure of 1 atm, we can see from the graph that the flow reaches an exit pressure of 1% atm when M=3.7

From the table, at Me=3.7, $\frac{\mathrm{To}}{\mathrm{Te}} = 3.738 \leftrightarrow \mathrm{Te} = \frac{894.622}{3.738} \leftrightarrow \mathrm{Te} = 239.33\mathrm{K} \simeq 240\mathrm{K}$

From equation $\mathrm{Me} = \frac{\mathrm{Ve}}{\sqrt{\gamma \mathrm{RTe}}}$, we can deduce that the flow velocity $\mathrm{Ve2}$ at the exit of the second convergent-divergent nozzle will be equal to 1148.979m/s for $\mathrm{Me2} = 3.7\ \ \mathrm{Te2} = 240\mathrm{K}$.

The temperature and pressure at the exit of the second nozzles are identical, so the density of the air at the exit of the second nozzle will also be the same ($\rho\mathrm{e} = 1.47 * 10^{-5}\ \mathrm{kg}/m^3$).

At this stage of the process, the flow velocity will not be high enough to allow it to keep moving if a pressure of 101325 Pa builds up due to a re-compression stage. In this case, another compressor will therefore be required in order to increase the pressure of the flow and continue the cycle.

Using the parameters from this analysis, a compressor will therefore be needed for every two convergent-divergent nozzles. However, it is possible to reduce this frequency by varying certain parameters. For example, the mixing of the two different fluids have not been taken into considerations, but this mixing will increase the density of the resulting flow, which will therefore give him more momentum in order to keep moving. The gas selected for this analysis is air, however, other gases with more optimal thermodynamic properties could be considered. Furthermore, since the temperature drops with the expanding flow in the divergent section, the air has the chance of becoming liquefied. For that reason, preheating might be a highly considerable option. Finally, using solar panels to reconvert thermal energy into electrical power might be an interesting option as the system will require a significant amount of energy.

Further research and testing are required to come to a fully informed decision as to which of the discussed vacuum systems is best for the full-scale integration of an Hyperloop system. Small scale modelling of these vacuum systems would provide more insights into how detrimental the predicted losses are during degassing.

5. Bibliography

Analysis of Over-Ground vs Under-Ground Tunnel Design Challenges and Risks

[1] 'The Effects of Soil Type on Earthquake Damage | WSRB Blog'. https://www1.wsrb.com/blog/the-effects-of-soil-type-on-earthquake-damage (accessed Apr. 26, 2023).

[2] 'The environmental implications of Hyperloop', *STOUT MEP*, Jul. 27, 2020. https://www.stoutmep.com/electromechanical-ethos-blog/the-environmental-implications-of-Hyperloop (accessed Apr. 26, 2023).

[3] E. Chiland, 'Is it safe to build tunnels in earthquake-prone Los Angeles?', *Curbed LA*, Jan. 16, 2019. https://la.curbed.com/2019/1/16/18178979/subway-tunnels-earthquake-fault-lines (accessed Apr. 26, 2023).

[4] D. Hyperloop, 'The Underground Potential of the Hyperloop system', *Hyperloop Connected*, Apr. 02, 2018. https://Hyperloopconnected.org/2018/04/the-underground-potential-of-the-Hyperloop-system/ (accessed Apr. 26, 2023).

[5] P. Thompson, 'A SCIENTIFIC AND ECONOMIC ANALYSIS OF THE HYPERLOOP AS IT PERTAINS TO MASS TRANSPORTATION'.

[6] R. Walker, 'Hyperloop : Cutting through the hype', [Online]. Available: https://trl.co.uk/uploads/trl/documents/ACA003-Hyperloop.pdf

[7] 'ET3GenericProposal013au.pdf'. Accessed: Apr. 26, 2023. [Online]. Available: http://et3.nl/images/upload/file/ET3GenericProposal013au.pdf

[8] 'Thompson - A SCIENTIFIC AND ECONOMIC ANALYSIS OF THE HYPERLOO.pdf'. Accessed: Apr. 26, 2023. [Online]. Available: https://etd.ohiolink.edu/apexprod/rws_etd/send_file/send?accession=case1560510307453676&disposition=inline

The Kantrowitz Limit

[1]
A. Bose and V. K. Viswanathan, "Mitigating the Piston Effect in High-Speed Hyperloop Transportation: A Study on the Use of Aerofoils," *Energies*, vol. 14, no. 2, p. 464, Jan. 2021, doi: https://doi.org/10.3390/en14020464.

[2]
M. M. J. Opgenoord and P. C. Caplan, "Aerodynamic Design of the Hyperloop Concept," *AIAA Journal*, vol. 56, no. 11, pp. 4261–4270, Nov. 2018, doi: https://doi.org/10.2514/1.j057103.

[3]

M. Bizzozero, Y. Sato, and M. A. Sayed, “Aerodynamic study of a Hyperloop pod equipped with compressor to overcome the Kantrowitz limit,” *Journal of Wind Engineering and Industrial Aerodynamics*, vol. 218, p. 104784, Nov. 2021, doi: https://doi.org/10.1016/j.jweia.2021.104784.

Tunnel Materials Selection

Ductile to Brittle Transition & Vacuum Buckling

[1] H.-K. Kim, ‘Uncertainties of the critical buckling pressure of a tube’, *Procedia Structural Integrity*, vol. 5, pp. 63–68, Jan. 2017, doi: 10.1016/j.prostr.2017.07.064.

[2] ‘Tanks and Vessels’, *Dodman Limited*. https://www.dodman.com/tanks-and-vessels/ [accessed Apr. 23, 2023].

[3] ‘Factors of Safety’. https://www.engineeringtoolbox.com/factors-safety-fos-d_1624.html [accessed Apr. 23, 2023].

[4] C. Hauviller, ‘Design rules for vacuum chambers’, *CERN*, pp. 31–42, 2007. https://cds.cern.ch/record/1046848/files/p31.pdf [accessed Apr. 2023].

[5] ‘Overview of materials for Low Alloy Steel’. https://www.matweb.com/search/DataSheet.aspx?MatGUID=d1bdbccde4da4da4a9dbb8918d783b29&ckck=1 [accessed Apr. 23, 2023].

[6] ‘Ductile to brittle failure transition of HSLA-100 Steel at high strain rates and subzero temperatures | Elsevier Enhanced Reader’. https://reader.elsevier.com/reader/sd/pii/S0013794416300790?token=9EDCD0D7056CEE925B921FB3D5BE46ED998EDDAA636BEE592C26B8E684EC1F73722F7F251BD294389ECFB3128538AF78&originRegion=eu-west-1&originCreation=20230423131951 [accessed Apr. 23, 2023].

Tunnel Materials

[1] J. Riley *et al.*, ‘2002 Davis-Besse Reactor Pressure Vessel Head Degradation Knowledge Management Digest’. Office of Nuclear Regulatory Research, Feb. 2014. Accessed: Apr. 04, 2023. [Online]. Available: https://www.nrc.gov/docs/ML1403/ML14038A119.pdf

[2] ‘Corr Science » Principles of Corrosion’. http://www.corrscience.com/products/corrosion/intro-to-corrosion/principles-of-corrosion/ [accessed Apr. 19, 2023].

[3] W. D. Jr. Callister and D. G. Rethwisch, *Materials Science and Engineering*, 9th ed. Wiley, 2014.

[4] I. Matsushima, '43. Carbon Steel - Atmospheric Corrosion', in *Uhlig's Corrosion Handbook*, 3rd ed.John Wiley & Sons, pp. 579–589. Accessed: Apr. 19, 2023. [Online]. Available: https://app.knovel.com/hotlink/pdf/id:kt008TZ752/uhlig-s-corrosion-handbook/failure-analysis-procedures

[5] 'AISI 304 Stainless Steel vs. ASTM A242 HSLA Steel :: MakeItFrom.com'. https://www.makeitfrom.com/compare/AISI-304-S30400-Stainless-Steel/ASTM-A242-HSLA-Steel [accessed Apr. 19, 2023].

[6] P. R. Khaladkar, '66. Using Plastics, Elastomers, and Composites for Corrosion Control', in *Uhlig's Corrosion Handbook*, 3rd ed.John Wiley & Sons, pp. 915–971. Accessed: Apr. 19, 2023. [Online]. Available: https://app.knovel.com/hotlink/pdf/id:kt008TZ752/uhlig-s-corrosion-handbook/failure-analysis-procedures

[7] 'Polyimide', *Wikipedia*. Mar. 17, 2023. Accessed: Apr. 19, 2023. [Online]. Available: https://en.wikipedia.org/w/index.php?title=Polyimide&oldid=1145101307

[8] 'Tunnels and underground structures', *LKAB Minerals*. https://www.lkabminerals.com/product-application/tunnels-and-underground-structures/ [accessed Apr. 19, 2023].

[9] M. S. Dixit and K. A. Patil, 'Study of Effect of Difference Parameters on Bearin Capacity of Soil', *Indian Geotechnical Society, GEOTID*, pp. 431–005, 2010.

Inducing and Maintaining a Vacuum

Rotary Vane Pumps

[1] 'Becker Vacuum Pumps, Compressors and Side Channel Blowers :: U 5.201'. https://www.becker-international.com/uk/1121/u-5.201.htm (accessed May 06, 2023).

[2] '[Hot Item] 5.5kw 200m3/H Rotary Vane Vacuum Pumps', *Made-in-China.com*. https://pransch.en.made-in-china.com/product/dwzThgkrAiVc/China-5-5kw-200m3-H-Rotary-Vane-Vacuum-Pumps.html (accessed May 06, 2023).

[3] 'Large Oil Sealed Rotary Vane Vacuum Pump for long and trouble free pump - Woosung Vacuum', *Woosung Vacuum Co., Ltd.*, Sep. 28, 2017. http://www.ws-vacuumpump.com/blog/portfolio-item/large-oil-sealed-rotary-vane-vacuum-pump/ (accessed May 06, 2023).

[4] *Vacuum Pumps Explained - Basic working principle HVAC*, (Oct. 02, 2019). Accessed: May 06, 2023. [Online Video]. Available: https://www.youtube.com/watch?v=pnqXEnn3DNk

[5] *Pump Down Times - Vacuum Pump, Equation & Examples*, (Jan. 02, 2020). Accessed: May 06, 2023. [Online Video]. Available: https://www.youtube.com/watch?v=bb7E2HAIqp4

[6] ‘Check Valve - How They Work’, *Tameson.com*. https://tameson.com/pages/check-valves (accessed May 06, 2023).

Novel Design Approach

[1] V. T. Group part of the Atlas Copco, ‘The Fundamentals of Vacuum Science - Vacuum Science World’. https://www.vacuumscienceworld.com/vacuum-science (accessed May 06, 2023).

[2] *Steam Jet Ejectors*, (Dec. 04, 2018). Accessed: May 06, 2023. [Online Video]. Available: https://www.youtube.com/watch?v=N-1MrAABFIA

[3] ‘Oups…’, *Shutterstock*. https://www.shutterstock.com/fr/image-photo/exhaust-jet-fighter-engine-2288417687 (accessed May 06, 2023).

[4] ‘Comparison of novel variable area convergent-divergent nozzle performances obtained by analytic, computational and experimental methods | Elsevier Enhanced Reader’. https://reader.elsevier.com/reader/sd/pii/S0307904X18300283?token=CB79FE2B6F6659FA398E90F14244CD9FDFCE2A8D3BD83035FCA5A6694A8413BB294BAE8C77418294BB215013858219FD&originRegion=eu-west-1&originCreation=20230506140245 (accessed May 06, 2023).

6. Appendices

Appendix A.1

The thickness of polymeric coating on the exterior of the tunnel will require further research. Required corrosion resistance and therefore barrier thickness will be specific to the environment, and therefore, may need to be fine-tuned depending on where the full-scale system is being integrated.

Appendix A.2

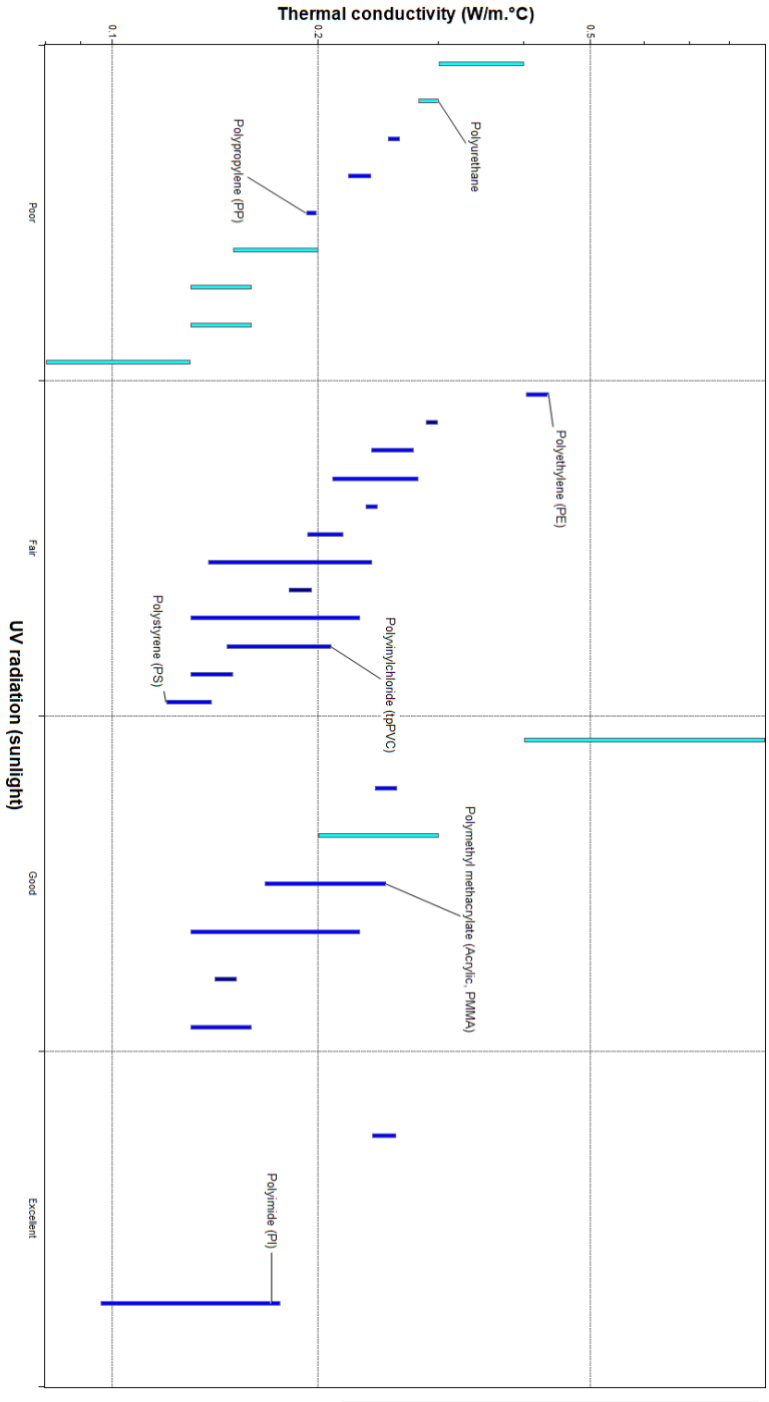

Appendix A.3

Further research is required to find the ideal processing route and application method the optimise the functional properties of the insulative and corrosion protective barrier.

Appendix A.4

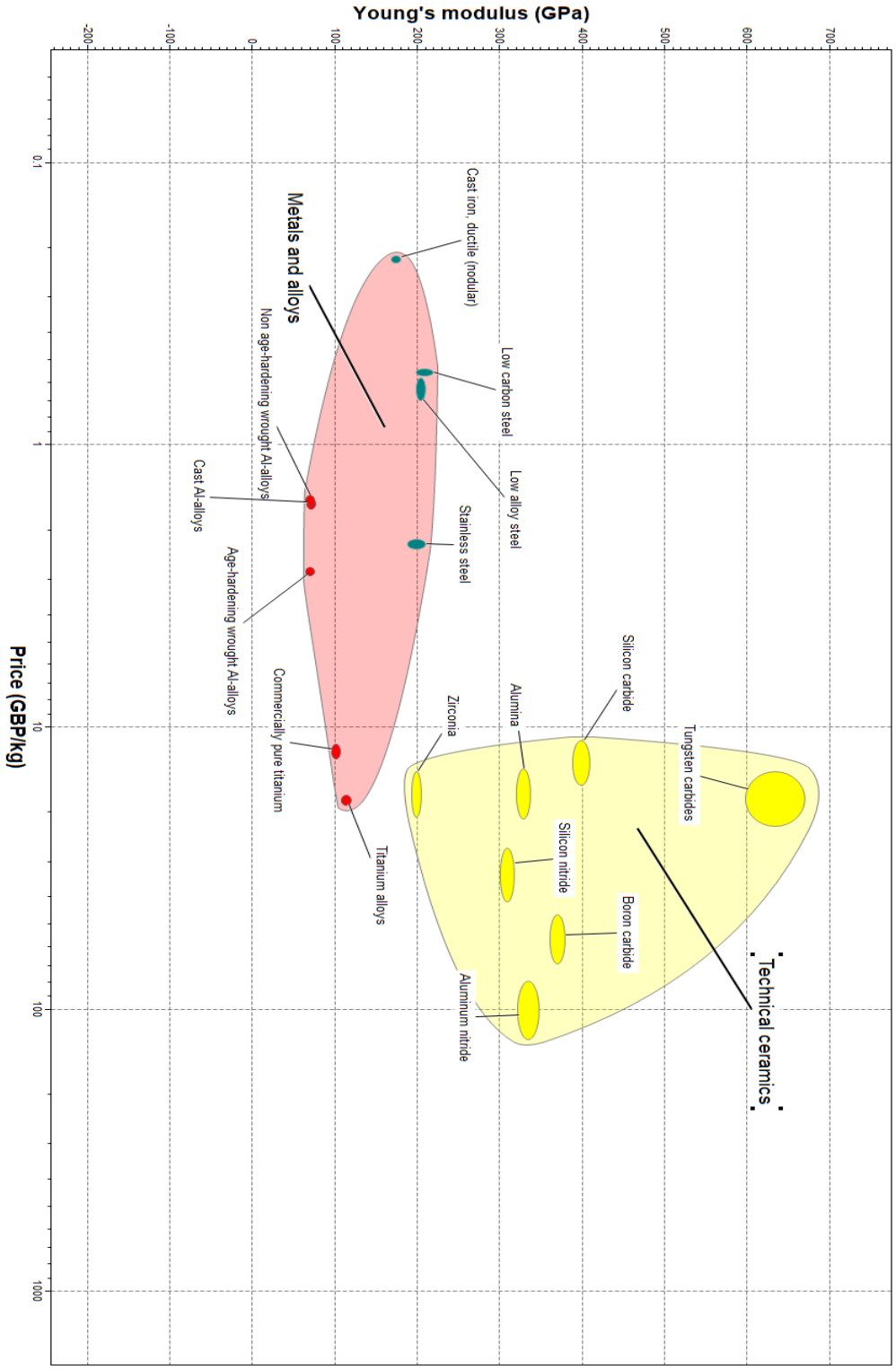

Appendix A.5

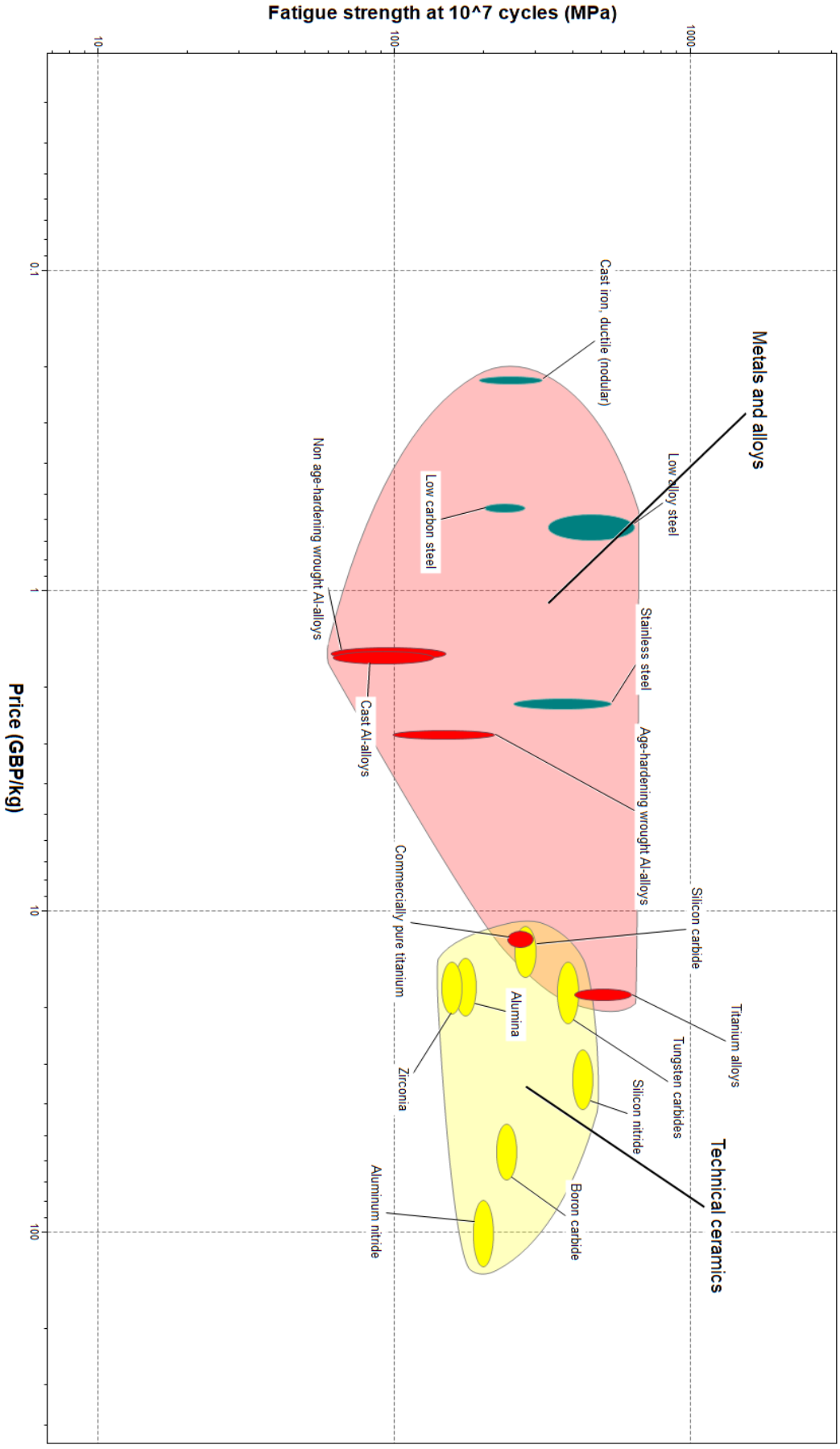
Fatigue strength at 10^7 cycles (MPa)
10
100
1000
Price (GBP/kg)
0.1
1
10
100
Metals and alloys
Cast iron, ductile (nodular)
Low alloy steel
Low carbon steel
Non age-hardening wrought Al-alloys
Stainless steel
Cast Al-alloys
Age-hardening wrought Al-alloys
Commercially pure titanium
Silicon carbide
Titanium alloys
Alumina
Tungsten carbides
Zirconia
Silicon nitride
Technical ceramics
Aluminum nitride
Boron carbide

Appendix B.1

To account for uncertainty and variations in properties between steel samples, the minimum Young's modulus (E) and maximum Poisson's ratio (ν) were used to calculate the required thickness for the tunnel to find a lower bound. As can be found on the source material, both of these values exist within a range. E lies between 300-500 MPa, and ν, between 0.270-0.300.

Appendix B.2

Calculation to find minimum required tunnel thickness:

$$\rho_{cr} = \frac{0.25E}{1-\nu^2}\left(\frac{t}{R}\right)^3 \quad (4)$$

$$t = \left[\sqrt[3]{(\rho \times safety\ factor)\frac{(1-\nu^2)}{0.25E}}\right]R$$

$$t = \left[\sqrt[3]{\frac{(10132500\times4)(1-0.300^2)}{0.25(183\times10^9)}}\right]0.75$$

$t = 0.1396\ m$
$\boldsymbol{t = 13.96\ cm}$

Appendix C.1

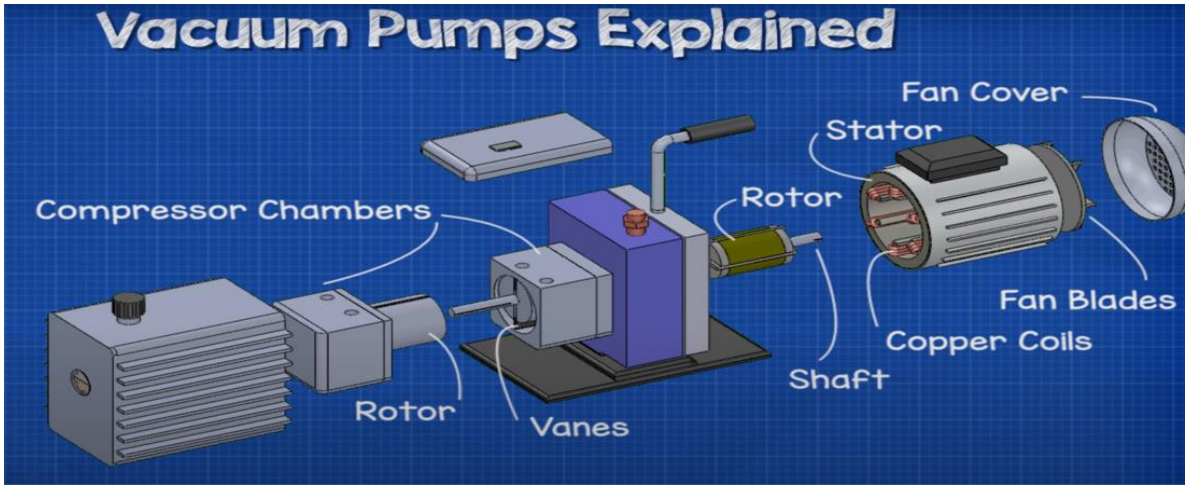

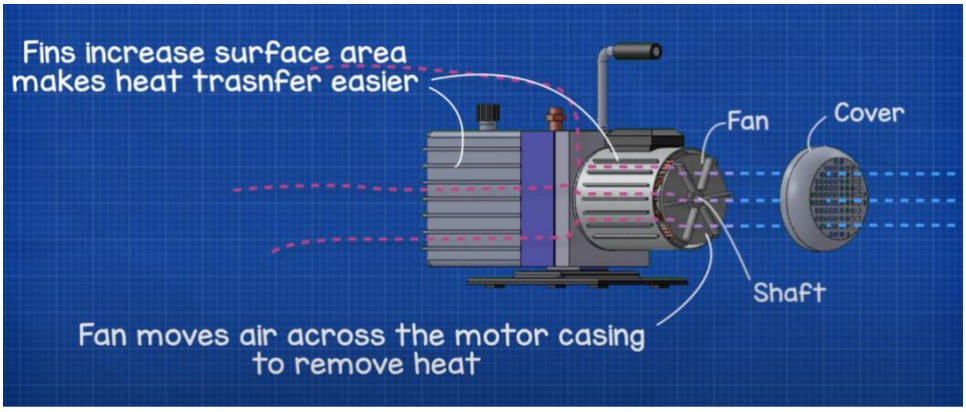
Fins increase surface area
makes heat trasnfer easier
Fan
Cover
Shaft
Fan moves air across the motor casing
to remove heat

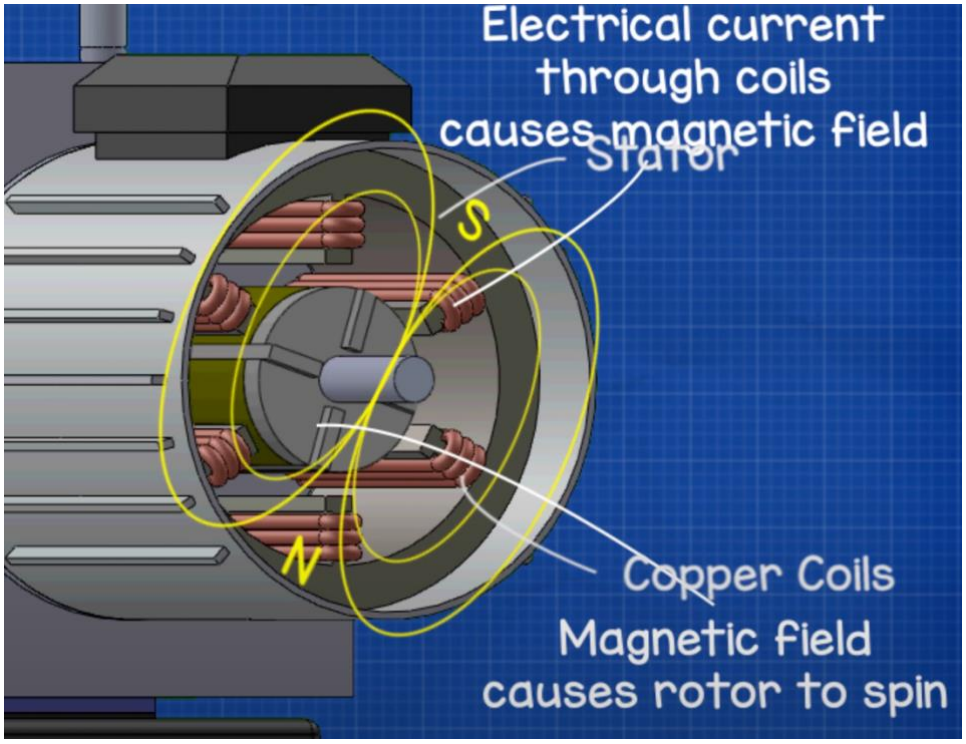
Electrical current
through coils
causes magnetic field
Stator
S
N
Copper Coils
Magnetic field
causes rotor to spin

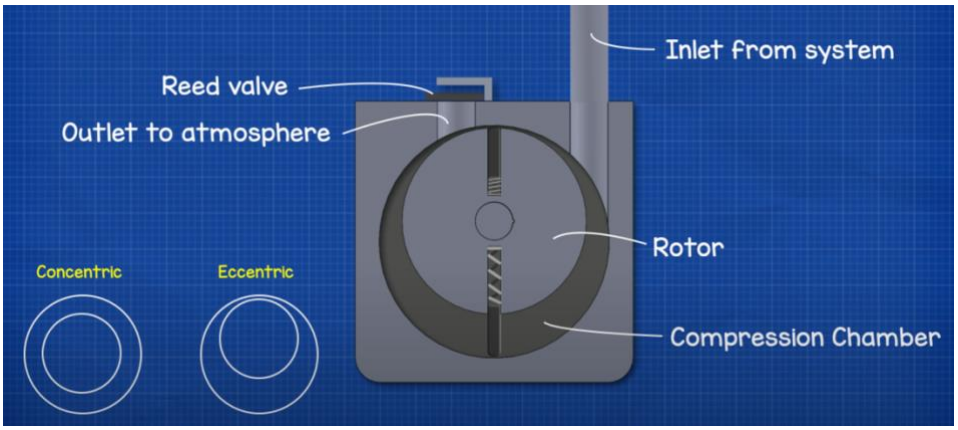
Inlet from system
Reed valve
Outlet to atmosphere
Rotor
Concentric
Eccentric
Compression Chamber

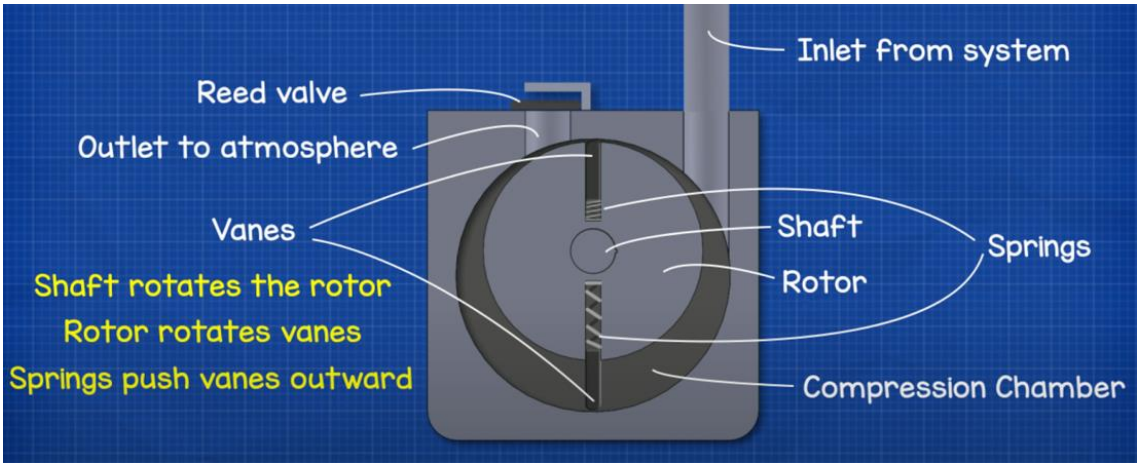
Inlet from system
Reed valve
Outlet to atmosphere
Vanes
Shaft rotates the rotor
Rotor rotates vanes
Springs push vanes outward
Shaft
Springs
Rotor
Compression Chamber

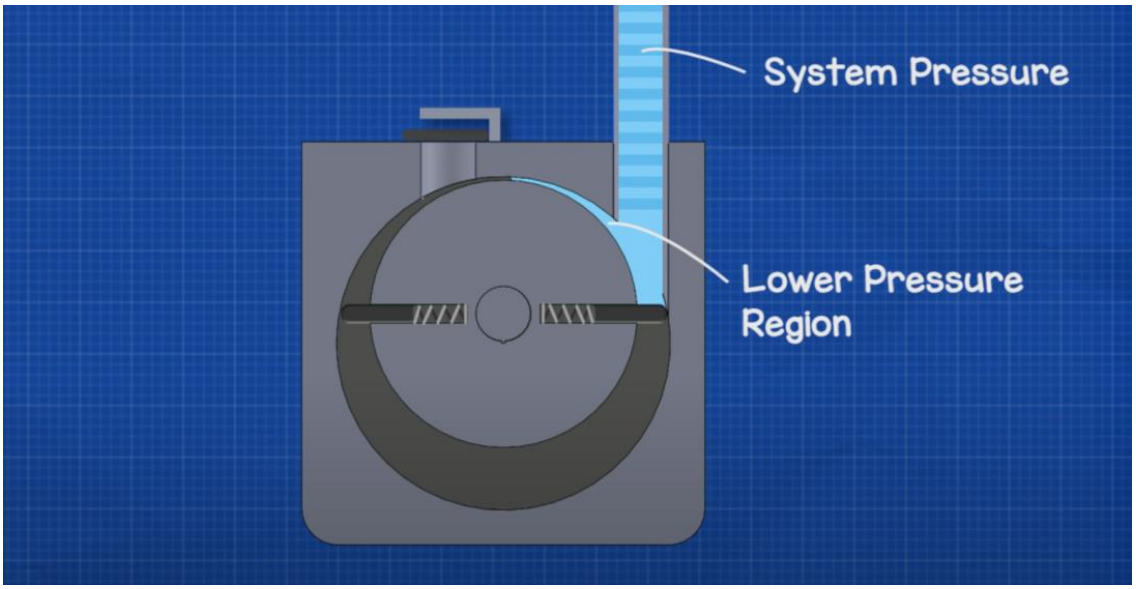
System Pressure
Lower Pressure Region

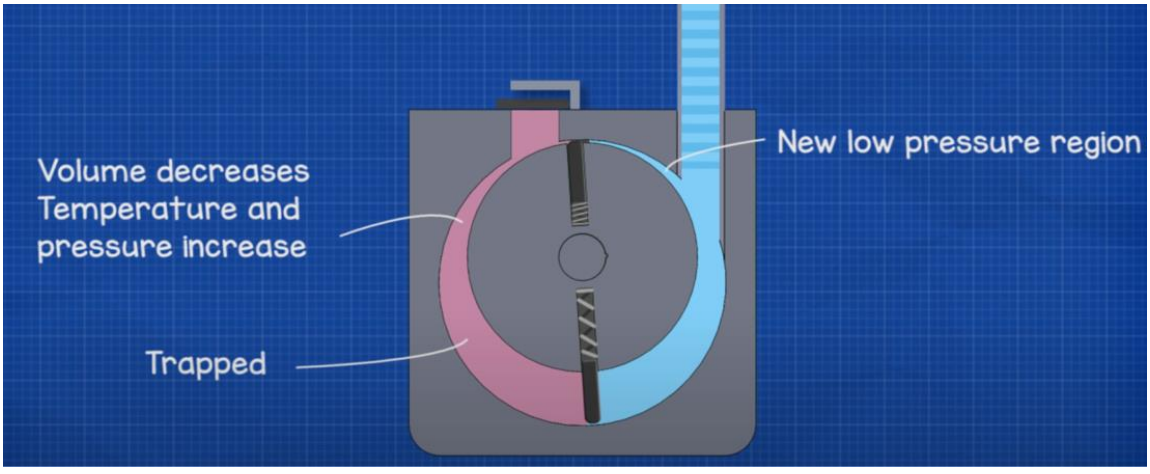
Volume decreases
Temperature and pressure increase
Trapped
New low pressure region

Appendix C.2

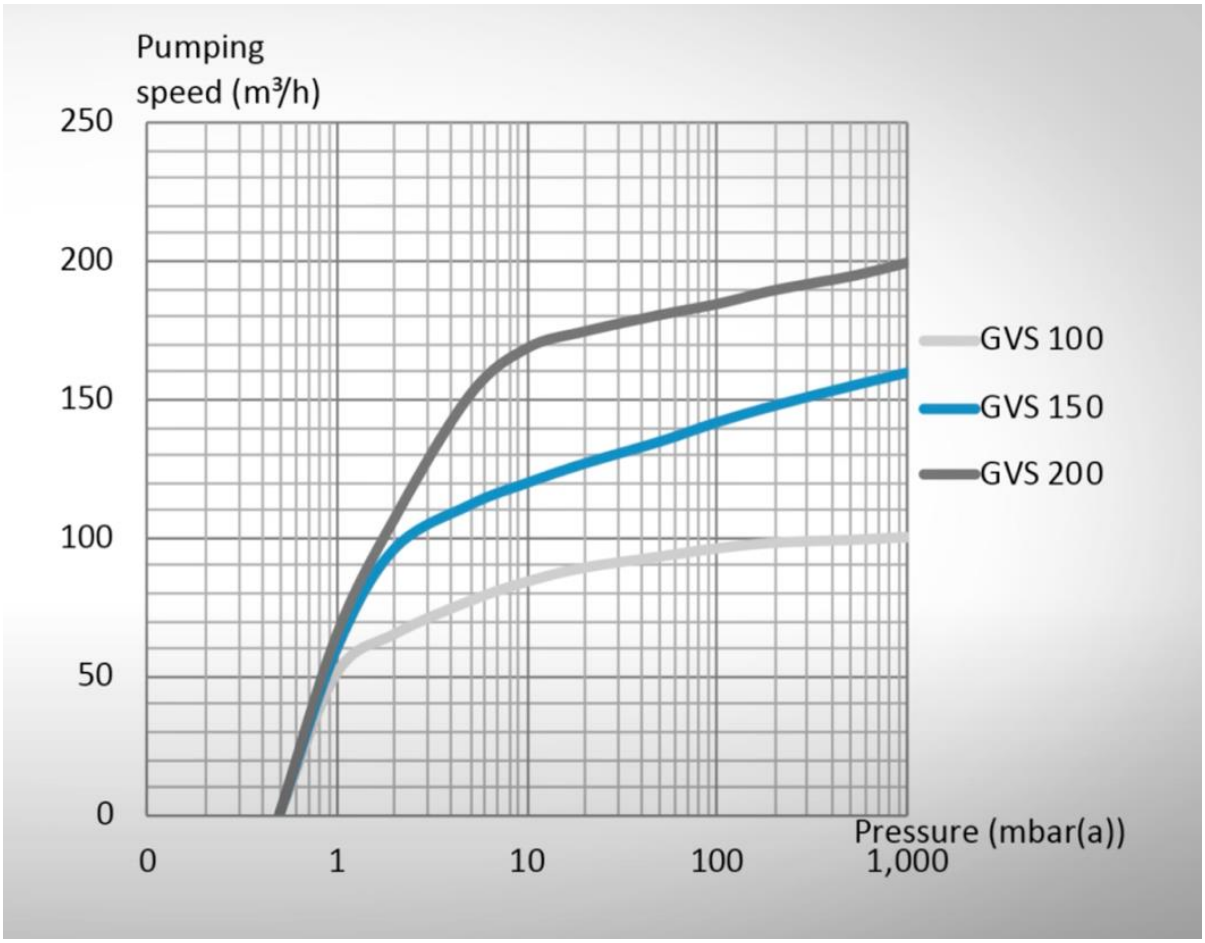
Pumping
speed (m³/h)
250
200
150
100
50
0
0
1
10
100
1,000
Pressure (mbar(a))
GVS 100
GVS 150
GVS 200